Quantum Linearity from Gravitational Record Erasure

Hong Zhang

May 2026

Abstract

Quantum linearity is usually postulated rather than derived. We ask: under what microscopic conditions on a quantum-gravity regulator does linearity follow from the erasure structure of gravitational records? Two results are established. A *no-go theorem* shows that gravitational records and primitive erasure do not by themselves enforce linearity: a stationary nonlinear anomaly can always be constructed unless a microscopic Ward, modular, or constraint identity removes it. A *conditional closure theorem* then shows that, if a finite regulator satisfies five conditions—a projective record system, a uniform erasure resolvent, stationary anomaly cancellation, transport-exactness, and a bounded contracting homotopy for a two-term Koszul causal complex—the record-erased operational dynamics converges to an affine quantum channel with an explicit error bound. All five conditions are instantiated in four quantum-gravity regulators: JT gravity (via the $\mathrm{SL}(2,\mathbb{R})$ Schwarzian Ward identity on the non-identity primary sector), an AdS–Rindler entanglement wedge (via the JLMS first law), a finite-cutoff holographic operator-algebra code (via the gauge–logical dichotomy), and a spin-network corner (via Peter–Weyl averaging, subject to an explicit singlet-exclusion assumption). This is not a derivation of linearity for the real universe; it is a finite-regulator conditional theorem that reduces quantum linearity to a checkable list of microscopic identities.

Contents

1 Introduction

Quantum mechanics is linear: an operationally allowed evolution of states is an affine map on density matrices, given by a completely positive trace-preserving channel. This linearity is usually treated as an independent postulate, not a derived consequence of any deeper principle. Yet attempts to relax it run into a sharp obstruction: almost every deterministic nonlinear modification of quantum dynamics either generates superluminal signaling between entangled subsystems or violates the structure of mixed states. Weinberg's nonlinear extension of quantum mechanics [1] was shown by Gisin and Polchinski to permit such signaling in EPR-type configurations [2, 3]. Simon, Bužek, and Gisin sharpened the no-signaling constraint to a general statement about admissible deterministic dynamics [4], and recent analyses extend the discussion to cosmological and gravitational settings [5]. The conclusion of this line of work is that nonlinearity is not free: an additional mechanism is needed to prevent the nonlinearity from being observable.

A natural source of such a mechanism is the gravitational sector. In a quantum theory of gravity, local preparations are not passive: they couple to gravitational degrees of freedom and leave physical records — edge modes, boundary charges, corner data, holographic codewords — in the gauge or boundary sector of the theory [6, 7]. If these records are then erased by an environmental or modular relaxation, the operational dynamics seen by a distant observer is the record-averaged one. This averaging is precisely the kind of operation that can hide a controlled nonlinearity: a state-dependent response that depends on the record can disappear from the averaged dynamics, provided the response is suitably structured.

This paper formalizes the mechanism as *Causal Preparation Erasure* (CPE). The core technical claim is that, in a finite gravitational-record sector with a primitive erasure generator K, a nonlinear response $\mathcal{N}_r$ indexed by records r is invisible in the record-erased dynamics if and only if it is a coboundary $\mathcal{N} = KG$ for some potential G. By a standard finite Markov-chain Fredholm alternative, this coboundary condition is equivalent to a stationary centering condition $\sum_r \mu_r \mathcal{N}_r = 0$, where μ

is the stationary record distribution. The CPE mechanism therefore reduces the question "which nonlinearities are causal?" to the question "which microscopic gravitational identities enforce the centering condition?".

We prove two results.

No-go theorem (§2). Records, primitive erasure, and split-local support do not by themselves imply linearity. A stationary, split-local, state-dependent functional can always be added to the dynamics without changing the record system, the erasure generator, or the support structure. This functional fails the centering condition and produces a persistent nonlinear drift in the erased dynamics. Therefore a microscopic Ward, BRST, modular, or constraint identity must be invoked to eliminate it. The no-go theorem identifies what cannot be derived from the CPE structure alone.

Conditional closure theorem (§4). If the gravitational regulator supplies assumptions (A1)–(A5) — a finite projective record system, a uniform zero-mean erasure resolvent, stationary anomaly cancellation derived from a microscopic identity, a transport-exact coboundary potential, and a bounded contracting homotopy for the causal double complex — then record-erased operational dynamics converges to an affine quantum channel with an explicit, model-independent error bound. The bound is a sum of four terms: a projective coarse-graining residual, a stationary-anomaly residual, a transport-defect residual, and an initial-final record disequilibrium boundary term. Each residual is zero in the corresponding limit.

Theorem 2 is a conditional abstract result: it shows that *if* (A1)–(A5) hold, *then* the error bound follows by Poisson algebra, spectral-gap estimates, and homological perturbation. The physical substance of CPE is not in this implication, but in whether a given quantum-gravity regulator satisfies (A1)–(A5). The Markov generator K in condition (A2) is a *model input*; the centering identity in (A3) must be derived from a specific microscopic symmetry in each regulator; and (A4)–(A5) impose transport and cohomological constraints that are instantiated here only at finite cutoff λ. The body of the paper shows that all five conditions can be simultaneously instantiated in four concrete regulators, and identifies what remains open in each.

One main worked regulator + three further regulators in appendices. The body of the paper develops JT gravity (§5) as the main worked regulator. Records are carried by Schwarzian boundary energy and horizon-dilaton bins [8–10]; the stationary anomaly cancellation is derived from the $\mathrm{SL}(2,\mathbb{R})$ Ward identity of the Schwarzian on the non-identity primary sector (§5.5); and one bath-induced Davies/van Hove realization of the Markov erasure rates is constructed from a system–bath Hamiltonian via the weak-coupling limit (§5.4), with the specific rates treated as model inputs. Three further regulators are constructed in the appendices, each in less detail but following the same template: AdS–Rindler entanglement wedges (Appendix A), with first-law/JLMS [11–14] replacing the Ward identity; finite-cutoff operator-algebra AdS/CFT codes (Appendix B), with the gauge–logical dichotomy [15–17] replacing it; and spin-network/corner quantizations (Appendix C), with the Gauss/closure constraint and Peter–Weyl [7, 18–21]. In each model we exhibit the record algebra, state the erasure generator with its microscopic origin (including the physical inputs that are taken as modelling data), derive the stationary anomaly condition from a specific microscopic identity, solve the finite Poisson equation, bound the transport defect, and construct an explicit contracting homotopy for the causal double complex. The structural unity of the four constructions — all instances of the same abstract template — is a feature, not a defect; §6 makes this explicit in a side-by-side comparison table. None of the four regulators claims to describe the real universe; each

is a finite-cutoff prototype that instantiates (A1)–(A5) and identifies which conditions follow from first principles and which are modelling inputs.

Relation to standard decoherence theory. The CPE mechanism shares architectural features with environmental decoherence [22–24]: in both, an environment (here, the gravitational record sector) couples to system degrees of freedom, and the resulting reduced dynamics is the environment-averaged one. The crucial difference is what is averaged. Standard decoherence suppresses off-diagonal density-matrix elements in a preferred (pointer) basis, leading to an effective *classical* probability distribution but leaving the system dynamics linear in ρ. CPE instead asks when a *nonlinear* system response can be hidden by the same averaging. The answer is: only if the response is a K-coboundary of the record generator. This coboundary structure — not present in standard decoherence theory, where there is no nonlinear response to average over — is what makes CPE a genuine derivation of linearity rather than a special case of decoherence. In particular, the no-go theorem (Theorem 1 below) is specific to the nonlinear case: it says that decoherence-like erasure structure alone is insufficient to suppress nonlinearity, in contrast to the linear case where decoherence alone does suppress quantum interference.

Scope. The closure conditions are physically meaningful, mutually compatible, and individually instantiable inside concrete quantum-gravity regulators. In particular, the persistence of a single stationary anomaly in any candidate regulator would, by the no-go theorem, defeat the mechanism in that regulator. CPE converts the question of low-energy quantum linearity into a finite list of microscopic identities, each of which a candidate theory of quantum gravity may satisfy or fail.

Organization. Section 2 states the CPE data tuple and the no-go theorem. Section 3 proves the finite-record Poisson/coboundary lemma and the conductance estimate, including a worked three-state numerical illustration (§3.5). Section 4 states and proves the general closure theorem. Section 5 constructs the main worked regulator (JT gravity). Section 6 compares the structural ingredients of all four closures (one in the body, three in appendices) in a side-by-side table. Section 7 develops the SYK/JT analog-simulator target as a simulation protocol with explicit discrimination criterion. Section 8 summarizes what has been proved and identifies the remaining model-dependent questions. Appendices A–C construct the three further worked regulators (AdS–Rindler entanglement wedge, finite-cutoff AdS/CFT operator-algebra code, spin-network/corner quantization) in the same template as §5.

Reading guide. Different readers may prefer different entry points. A reader interested primarily in *the abstract mechanism* can read §2–4 and stop there: the conditional closure theorem, the no-go theorem, and the cohomological framework are complete in those three sections. A reader who wants *the gravitational worked model first* should proceed directly to §5 (JT gravity) after §4. A reader who prefers *the cleanest finite-dimensional instantiation*, in which every step is a closed problem in finite linear algebra and operator-algebra QEC, should read Appendix B (AdS/CFT operator-algebra code) before §5; the operator-algebra setting makes the gauge–logical dichotomy transparent without the gravitational interpretation. Appendices A and C (AdS–Rindler and spin-network corners) are the remaining two instantiations of the same template and may be read independently.

2 The CPE data tuple, no-go theorem, and closure schema

The central claim of CPE is not that arbitrary deterministic nonlinear quantum mechanics is causal. It is the narrower claim that a deterministic nonlinear response can be compatible with no-signaling if it is a coboundary in a local, erasing record sector. When the record is equilibrated or discarded, the coboundary contributes only boundary terms, and the effective operational dynamics is affine-linear in the density matrix. The theory becomes physically explanatory only when the record sector and its erasure are derived from a microscopic gravitational model.

2.1 The data tuple

Definition 1 (CPE data tuple at cutoff λ)**.** A *CPE data tuple* at cutoff scale λ is a sextuple

$$\boxed{\mathfrak{D}_\lambda = (R_\lambda, \mathfrak{Z}_\lambda, K_\lambda, \mu_\lambda, \mathcal{N}_\lambda, Q_\lambda)} \tag{1}$$

where:

- R_λ is a finite set of *record labels*, indexing equivalence classes of microscopic boundary or edge configurations distinguishable at resolution λ;
- $\mathfrak{Z}_\lambda \simeq \ell^\infty(R_\lambda)$ is the abelian *record algebra* of bounded functions on R_λ, generated by the projectors Z_r onto each record class;
- $K_\lambda \in \mathrm{End}(\mathfrak{Z}_\lambda^*)$ is a primitive Markov generator acting on the dual (probability) side, encoding the erasure dynamics induced by environmental, modular, or constraint relaxation;
- $\mu_\lambda \in \mathfrak{Z}_\lambda^*$ is the unique stationary distribution, $\mu_\lambda K_\lambda = 0$, with $\mu_\lambda(r) > 0$ for all r;
- $\mathcal{N}_\lambda : \mathrm{End}(\mathcal{H}) \to \mathfrak{Z}_\lambda \otimes \mathrm{End}(\mathcal{H})$ is the *state-dependent nonlinear response*, encoding the proposed nonlinearity as a record-indexed family of (possibly state-dependent) maps;
- Q_λ is the differential of the *causal* L_∞ *complex* on the regulated foliation, controlling foliation curvature and the consistency of local glueings.

2.2 Definition of CPE-causal nonlinearity

Definition 2 (CPE-causal nonlinear response)**.** A nonlinear response $\mathcal{N}_\lambda$ is *CPE-causal* at cutoff λ if there exists a record-indexed potential $\mathcal{G}_\lambda$ such that

$$\mathcal{N}_\lambda = K_\lambda \, \mathcal{G}_\lambda \qquad \text{on each state argument.} \tag{2}$$

The condition (2) says that $\mathcal{N}_\lambda$ is a K_λ-coboundary: it lies in the image of the Markov generator viewed as a differential on the record algebra. The physical content is that $\mathcal{N}_\lambda$ disappears from the record-erased operational dynamics up to boundary terms, because $\int_0^T \nu_t(K_\lambda \mathcal{G}_\lambda)\,\mathrm{d}t$ telescopes after integration by parts against the Markov evolution $\dot{\nu}_t = \nu_t K_\lambda$. The precise statement and quantitative error bound are the content of Theorem 2 below.

2.3 No-go theorem: structure alone does not imply linearity

The first result is a structural obstruction: the existence of records, of a primitive erasure generator, and of split-local support for $\mathcal{N}_\lambda$ is *not* sufficient to force $\mathcal{N}_\lambda$ to be CPE-causal.

Theorem 1 (No-go: CPE structure underdetermines linearity)**.** *Let $\mathfrak{D}_\lambda = (R_\lambda, \mathfrak{Z}_\lambda, K_\lambda, \mu_\lambda, \mathcal{N}_\lambda, Q_\lambda)$ be any CPE data tuple in which $\mathcal{N}_\lambda$ is CPE-causal, $\mathcal{N}_\lambda = K_\lambda \mathcal{G}_\lambda$. Let A be any bounded, split-local, state-dependent functional on* $\mathrm{End}(\mathcal{H})$ *with $A[\omega] \neq 0$ for some state ω. Then the modified response*

$$\widetilde{\mathcal{N}}_{\lambda,r}[\omega] := \mathcal{N}_{\lambda,r}[\omega] \;+\; A[\omega]\,\mathbf{1}_{\mathfrak{Z}_\lambda} \tag{3}$$

satisfies:

(i) $\widetilde{\mathcal{N}}_\lambda$ has the same record support, the same split-locality structure, and the same erasure generator K_λ as $\mathcal{N}_\lambda$;

(ii) $\widetilde{\mathcal{N}}_\lambda$ is not *CPE-causal: $\Pi_{\mu_\lambda}\widetilde{\mathcal{N}}_\lambda[\omega] = A[\omega] \neq 0$, so $\widetilde{\mathcal{N}}_\lambda \notin \mathrm{Ran}\, K_\lambda$;*

(iii) the record-erased dynamics under $\widetilde{\mathcal{N}}_\lambda$ acquires a persistent nonlinear drift of order $\varepsilon\, A[\omega]\, T$ over time T.

In particular, the data $(R_\lambda, \mathfrak{Z}_\lambda, K_\lambda, \mu_\lambda)$ together with split-locality of the response do not by themselves imply that the record-erased dynamics is affine-linear.

Proof. Item (i) is immediate from the construction: the perturbation $A[\omega]\,\mathbf{1}_{\mathfrak{Z}_\lambda}$ is constant in r, so it inherits the support and locality structure of the constant function $\mathbf{1}$. For (ii), apply $\Pi_{\mu_\lambda} = \sum_r \mu_\lambda(r)(\cdot)_r$ to (3): the first term vanishes by hypothesis on $\mathcal{N}_\lambda$, and the second term yields $A[\omega]\sum_r \mu_\lambda(r) = A[\omega]$. Since $\mathrm{Ran}\, K_\lambda$ coincides with the zero-mean subspace (by Lemma 1 below), $\widetilde{\mathcal{N}}_\lambda \notin \mathrm{Ran}\, K_\lambda$. Item (iii) is the contrapositive of the error bound (30) in the proof of Theorem 2: the term $a_\lambda T$ with $a_\lambda = \sup_\omega \|\Pi_{\mu_\lambda}\widetilde{\mathcal{N}}_\lambda[\omega]\| = \sup_\omega |A[\omega]|$ does not vanish as λ refines, so the bound does not contract to zero. □

Remark 1 (Scope of the no-go theorem). The no-go theorem says that records and erasure provide the *ambient structure* in which CPE-causal nonlinearities can be discussed, but the structure alone does not constrain $\mathcal{N}_\lambda$ to be CPE-causal. The constant-shift perturbation $A[\omega]\,\mathbf{1}_{\mathfrak{Z}_\lambda}$ is the simplest stationary anomaly: it is invariant under K_λ, so erasure does not damp it. Eliminating such anomalies requires an additional input: a microscopic Ward identity (§5), modular thermodynamic identity (§A), gauge/logical decomposition (§B), or constraint-averaging principle (§C). The four worked regulators in this paper show how each kind of identity can be implemented.

2.4 The closure schema

In view of the no-go theorem, a successful microscopic regulator must supply an identity that forces the centering condition. Together with the four further technical conditions of Theorem 2, this yields the closure schema that Theorem 2 formalises. The five conditions of Theorem 2 are labelled **(A1)**–**(A5)** in that theorem; we preview them here in a concise form to set up the model sections:

$$\textbf{(A3)}\quad \Pi_{\mu_\lambda}\mathcal{N}_\lambda := \sum_{r\in R_\lambda} \mu_\lambda(r)\mathcal{N}_{\lambda,r} = 0 \quad \text{(stationary anomaly cancellation)}, \tag{4}$$

$$\mathcal{N}_\lambda = K_\lambda \mathcal{G}_\lambda \text{ then follows} \quad \text{(automatic from (A3) by Lemma 1)}, \tag{5}$$

$$\textbf{(A4)}\quad \dot{\mathcal{G}}_\lambda = K_\lambda \mathcal{H}_\lambda + B_\lambda, \qquad B_\lambda \to 0 \quad \text{(transport-exactness)}, \tag{6}$$

$$\textbf{(A5)}\quad H^n_{Q_\lambda} = 0 \text{ for } n \geq 1 \quad \text{with a bounded contracting homotopy} \quad \text{(bounded causal contraction)}. \tag{7}$$

Conditions (A1) (projective tightness) and (A2) (uniform erasure resolvent) are stated precisely in Theorem 2. Condition (4) = (A3) is the stationary Ward/anomaly condition, which must be derived

from a microscopic symmetry of each regulator; the coboundary structure (5) is then automatic by Lemma 1; (6) = (A4) controls slow drift of the potential along the flow; (7) = (A5) controls the higher-order Maurer–Cartan corrections from local glueing, and is verified via the Koszul bicomplex (Lemma 3, Remark 4) together with the cover-multiplicity input (A4′) below. Each worked model *instantiates* conditions (A1)–(A5) at finite λ and identifies which are derived from microscopic symmetries and which are domain restrictions or modelling inputs. The continuum limit $\lambda \to 0$ remains separate.

Cover-multiplicity input (A4′). The cohomology condition (7) is verified in each worked model via a bicomplex argument (cf. Remark 4 below) that combines a Čech good cover of the model's causal base with the two-term Koszul resolution of Lemma 3. The bicomplex construction requires the cover-multiplicity constant $C_{\mathrm{cov}} := \|s\|$ (the operator norm of the Čech contracting homotopy associated to a chosen good cover $\mathcal{U}$) to be a bounded combinatorial input. We state this explicitly as

(A4′). *The good cover $\mathcal{U}$ of the regulator's causal base has bounded nerve multiplicity $C_{\mathrm{cov}} < \infty$, with the bound depending only on the dimension and topology of the cover and not on the regulator scale λ.*

The bicomplex acyclicity bound (21) is then additive in C_{cov} and $1/\gamma$, not a quadratic contraction inequality. Assumption (A4′) is a property of the chosen cover, fixed once and for all; cover refinement does not in general reduce C_{cov}. For one-dimensional bases (JT) and finite-graph bases (code, spin-network), an explicit good cover with bounded C_{cov} is available by direct construction; for the AdS–Rindler wedge, $C_{\mathrm{cov}}^{\mathrm{Rindler}}$ is bounded by the combinatorial type of the chosen causally convex subwedge cover.

3 Finite-record Poisson lemma and conductance estimate

All four worked regulators reduce part of the proof to two finite Markov-chain identities: a Fredholm-type characterization of the range of the erasure generator (Lemma 1), and a conductance lower bound on the zero-mean spectral gap (Lemma 2). We state and prove both here so that the model sections can quote them as named results.

Let R be a finite set of record labels. A Markov generator K acts on row probability vectors by

$$\dot{\nu}_r = \sum_s \nu_s K_{sr}, \qquad K_{rs} \geq 0 \ (r \neq s), \qquad \sum_s K_{rs} = 0. \tag{8}$$

Assume K is *primitive*: there is a unique stationary distribution μ with $\mu K = 0$ and $\mu_r > 0$ for all $r \in R$. Equivalently, the off-diagonal graph of K is irreducible and aperiodic. Let $P_0 := I - \mathbf{1}\mu$ denote the projector to the zero-mean subspace $V_0 := \{v : \mu(v) = 0\}$ (here $\mathbf{1}$ is the constant function $r \mapsto 1$ and the row–vector product $\mathbf{1}\mu$ acts by $v \mapsto \mu(v)\mathbf{1}$).

3.1 Poisson lemma: range = zero-mean subspace

Lemma 1 (Finite Poisson/coboundary lemma)**.** *Let K be a primitive Markov generator on a finite set R with stationary distribution μ, and let $N = (N_r)_{r \in R}$ be a vector-valued response with values in a Banach space $\mathcal{X}$. Then*

$$\sum_r \mu_r N_r = 0 \quad \Longleftrightarrow \quad N = KG \tag{9}$$

for some $G : R \to \mathcal{X}$, where $(KG)_r := \sum_s K_{rs} G_s$ (acting on the columns). A canonical solution is

$$G = K^D N, \qquad K^D = -\int_0^\infty e^{tK} P_0 \, \mathrm{d}t, \tag{10}$$

called the Drazin inverse *or* deviation matrix *of K on the zero-mean subspace. It satisfies $KK^D P_0 = K^D K P_0 = P_0$ and $K^D \mathbf{1} = 0$.*

Proof. The primitivity of K guarantees that $\operatorname{Ker} K = \operatorname{span}\{\mathbf{1}\}$ on the column side and that the cokernel of K is spanned by μ on the row side; this is the Perron–Frobenius theorem for primitive Markov generators [25]. Hence the range of K acting on $\mathcal{X}$-valued functions is the zero-μ-mean subspace $V_0 \otimes \mathcal{X}$. Equation (9) is the resulting Fredholm alternative.

For the canonical solution: on V_0, the semigroup e^{tK} is contractive in $L^2(\mu)$ (and in any norm by equivalence of norms on a finite-dimensional space). Concretely, by Lemma 2 below there exist constants $M, \gamma > 0$ with $\left\| e^{tK} P_0 \right\| \le M e^{-\gamma t}$, so the integral in (10) converges absolutely. A direct computation gives $K(-\int_0^\infty e^{tK} P_0 \, \mathrm{d}t) = -[e^{tK} P_0]_0^\infty = P_0$ (the upper limit vanishes by the exponential bound). Hence $KK^D = P_0$ on the zero-mean subspace, so $G = K^D N$ solves $KG = N$ whenever $N \in V_0 \otimes \mathcal{X}$. □

3.2 Spectral gap from conductance

The Drazin inverse (10) is bounded if and only if the zero-mean semigroup contracts exponentially, with a uniform rate γ. For reversible chains this rate is controlled by a Cheeger-type *conductance* bound, which gives an effective handle on $\left\| K^D P_0 \right\|$ in each model.

Lemma 2 (Conductance bound on the zero-mean spectral gap)**.** *Let K be a primitive Markov generator on a finite set R with stationary distribution μ. Suppose K satisfies detailed balance with respect to μ, $\mu_r K_{rs} = \mu_s K_{sr}$, and define the conductance*

$$\Phi_K \;:=\; \min_{\substack{S \subset R \\ \mu(S) \le 1/2}} \frac{\sum_{r \in S,\, s \notin S} \mu_r K_{rs}}{\mu(S)}. \tag{11}$$

Then the zero-mean spectral gap of $-K$ on $L^2(\mu)$ satisfies

$$\gamma \;:=\; \inf_{f \in V_0,\, \|f\|_{L^2(\mu)} = 1} \langle f, (-K) f \rangle_{L^2(\mu)} \;\ge\; \tfrac{1}{2} \Phi_K^2, \tag{12}$$

and consequently

$$\left\| e^{tK} P_0 \right\|_{L^2(\mu) \to L^2(\mu)} \;\le\; e^{-\gamma t}, \qquad \left\| K^D P_0 \right\|_{L^2(\mu) \to L^2(\mu)} \;\le\; \frac{1}{\gamma} \;\le\; \frac{2}{\Phi_K^2}. \tag{13}$$

Proof. For a reversible Markov generator, K is self-adjoint on $L^2(\mu)$ with $\operatorname{Ker} K = \operatorname{span}\{\mathbf{1}\}$. The Dirichlet form is

$$\langle f, (-K) f \rangle_{L^2(\mu)} = \tfrac{1}{2} \sum_{r,s} \mu_r K_{rs} (f_s - f_r)^2. \tag{14}$$

The Cheeger inequality for reversible Markov chains [26, 27] states that the smallest nonzero eigenvalue γ of $-K$ obeys $\gamma \ge \frac{1}{2}\Phi_K^2$, where Φ_K is the conductance (11). Since γ is the variational infimum in (12), we obtain (12).

The semigroup bound in (13) follows by spectral calculus: $\left\|e^{tK}P_0\right\|_{L^2(\mu)} = e^{-\gamma t}$ on the zero-mean subspace. The Drazin bound is then $\left\|K^D P_0\right\|_{L^2(\mu)} = \left\|\int_0^\infty e^{tK}P_0\,\mathrm{d}t\right\| \le \int_0^\infty e^{-\gamma t}\,\mathrm{d}t = 1/\gamma$. □

Remark 2 (Non-reversible chains). For non-reversible primitive generators, the Cheeger inequality holds for the *additive reversibilization* $K_{\mathrm{sym}} := \frac{1}{2}(K + K^*)$, where K^* is the $L^2(\mu)$-adjoint. One has $\operatorname{Ran} K = \operatorname{Ran} K_{\mathrm{sym}}$ on the zero-mean subspace, but the contraction rate of e^{tK} may differ from that of $e^{tK_{\mathrm{sym}}}$ by a polynomial prefactor coming from non-normality. In each model below we specify whether the erasure generator is reversible; when it is not, we state the auxiliary bound used in place of (12). The qualitative conclusion — a uniform λ-independent γ — is required in either case. The reversibilization K_{sym} is used only as an auxiliary spectral tool in this remark; it does not appear in the cohomology construction of §3.3, which uses K directly via the two-term Koszul resolution.

3.3 Two-term Koszul resolution of the Markov coboundary

The cohomology argument in each worked regulator (§5.7, App. A.7, App. B.7, App. C.7) requires a contracting homotopy on a vertical record-complex. In the present finite-Markov setting, the natural such complex is a *two-term Koszul resolution*: a chain complex of length two with K as the only differential. This avoids the algebraic mismatch that a Markov generator K on the record space does not in general satisfy $K^2 = 0$ and therefore is not directly a cochain differential of a longer complex. The two-term framework sidesteps the issue: there is no C^2 component, and the condition $d^2 = 0$ is vacuous.

Lemma 3 (Two-term Koszul resolution of the Markov coboundary)**.** *Let K be a primitive Markov generator on a finite set R with stationary distribution μ, and let $V_0 \subset \mathbb{C}^R$ be the zero-mean subspace. Define the cochain complex of length two*

$$C^\bullet: \quad 0 \longrightarrow C^0 \xrightarrow{d=K} C^1 \longrightarrow 0, \qquad C^0 = C^1 = V_0, \tag{15}$$

with differential $d := K|_{V_0} : C^0 \to C^1$ and $C^q = 0$ for $q \notin \{0,1\}$. Then:

(i) The condition $d^2 = 0$ is vacuous: d^2 acts from C^0 to $C^2 = 0$.

(ii) The complex is acyclic: $H^0(C^\bullet) = \ker(K|_{V_0}) = 0$ and $H^1(C^\bullet) = \operatorname{coker}(K|_{V_0}) = 0$, since by Lemma 1 the restriction $K|_{V_0} : V_0 \to V_0$ is a bijection.

(iii) The contracting homotopy $h : C^\bullet \to C^{\bullet-1}$ defined by

$$h^1 := K^D|_{V_0} : C^1 \to C^0, \qquad h^q := 0 \text{ for } q \neq 1, \tag{16}$$

satisfies the standard contraction identity

$$h\,d + d\,h = \mathbf{1}_{V_0} \quad \text{on every } C^q. \tag{17}$$

(iv) The homotopy is bounded: $\|h\| = \left\|K^D|_{V_0}\right\| \le 1/\gamma$ in $L^2(\mu)$, where γ is the spectral gap of Lemma 2.

Proof. Item (i) is immediate. Item (ii) is Lemma 1 restated: primitivity gives $\ker K|_{V_0} = 0$, and $\operatorname{Ran} K = V_0$ gives coker $= 0$. For (iii), at $q = 0$:

$$(hd + dh)(x) = h^1(Kx) + 0 = K^D K\,x = P_0 x = x \quad \text{for } x \in V_0, \tag{18}$$

using $K^D K = P_0$ from (10) and the fact that $P_0|_{V_0} = \mathbf{1}_{V_0}$. At $q = 1$:

$$(hd + dh)(y) \;=\; 0 + K(K^D y) \;=\; KK^D\, y \;=\; P_0 y \;=\; y \quad \text{for } y \in V_0, \tag{19}$$

since $C^2 = 0$ kills the $h^2 d^1$ contribution. Item (iv) is the bound $\left\|K^D P_0\right\| \le 1/\gamma$ from (13). □

Remark 3 (Why the two-term complex is the right framework). A longer cochain complex with K as differential would require $K^2 = 0$, which is false for a generic Markov generator (in fact K^2 is typically negative-definite on V_0 for a reversible chain, by self-adjointness). Earlier attempts to make K play the role of a cochain differential by introducing a discrete graph gradient d_K on the record graph Γ_K (so that $d_K^2 = 0$ tautologically) require an auxiliary structure — weighted incidence operator, graph Laplacian $\Delta_K = d_K^* d_K$, and the identification of Δ_K with K_{sym} via the Hodge decomposition — that is correct only in the reversible case with a specific $L^2(\mu)$ inner product. Mixing this with the Drazin inverse K^D (which is the Markov-generator pseudo-inverse, distinct from the graph-Laplacian pseudo-inverse Δ_K^+) introduces inconsistencies that are visible at the level of which operator contracts the vertical complex.

Lemma 3 bypasses all of this. The vertical complex has length two; the only differential is K itself; the only contracting operator is K^D from Lemma 1; the Hodge identity (17) is a one-line consequence of $K^D K = KK^D = P_0$ on V_0. No graph Laplacian, no d_K^*, no reversibilization K_{sym} enters the cohomology construction in any of the worked regulators below.

Remark 4 (How Lemma 3 enters the worked models). Each of the four worked regulators below builds a bicomplex

$$\mathcal{B}^{p,q} \;:=\; \check{C}^p(\mathcal{U}) \otimes C^q, \qquad p \ge 0, \quad q \in \{0, 1\}, \tag{20}$$

where $\check{C}^\bullet(\mathcal{U})$ is the Čech complex of a finite good cover $\mathcal{U}$ of the model's causal base and $C^\bullet$ is the Koszul complex (15) of the model's Markov generator K_λ on $V_0(K_\lambda)$. The total differential $Q = \delta \otimes \mathbf{1} + (-1)^p \mathbf{1} \otimes d$ satisfies $Q^2 = 0$ because $\delta^2 = 0$, $d^2 = 0$ (vacuous, Lemma 3(i)), and the cross-terms cancel by the Koszul-sign convention.

Acyclicity. By Künneth, acyclicity of both factors on the relevant subspaces implies $H_Q^n = 0$ for $n \ge 0$ on V_0-valued cochains: $H_\delta^p(\check{C}^\bullet) = 0$ for $p \ge 1$ (good-cover contractibility) and $H^q(C^\bullet) = 0$ (Lemma 3(ii)).

Contracting homotopy and norm bound. A contracting homotopy H for the total complex exists (by acyclicity in a finite-dimensional setting) and is constructed from the Koszul component h (Lemma 3(iii), norm $\le 1/\gamma$) and the Čech component s (norm $\le C_{\mathrm{cov}}$) via the standard two-factor tensor construction [28, 29]. The resulting norm bound is

$$\|H\| \;\le\; \frac{1}{\gamma} \;+\; C_{\mathrm{cov}} \left(1 + \frac{\|K\|}{\gamma}\right), \tag{21}$$

where $C_{\mathrm{cov}} := \|s\|$ is the cover-multiplicity constant of (A4′) below and γ is the Cheeger gap. This is a strictly additive bound; no contraction inequality of the form $C_{\mathrm{cov}}^2/\gamma < 1$ is needed. Each model below establishes the corresponding bicomplex acyclicity via Künneth and quotes this bound; no model-specific spectral-sequence or HPL iteration is required.

3.4 Explicit potential on one-dimensional birth–death chains

For the one-dimensional energy or area chains that appear in three of the four models, the Drazin inverse admits a closed-form expression. Let $R = \{0, 1, \ldots, L\}$ and write upward rates $u_m = K_{m,m+1}$

and downward rates $d_m = K_{m,m-1}$. Define the edge current

$$J_m := \sum_{j=0}^{m} \mu_j N_j, \qquad m = 0, \dots, L-1. \tag{22}$$

The equation $KG = N$ is equivalent to

$$\mu_m u_m (G_{m+1} - G_m) = J_m, \tag{23}$$

so that, after fixing $G_0 = 0$,

$$G_m = \sum_{q=0}^{m-1} \frac{J_q}{\mu_q u_q}. \tag{24}$$

This formula will be used repeatedly in the model sections.

3.5 Numerical illustration: a three-state birth–death chain

To make the abstract finite-record mechanism concrete before the model sections, we work through the simplest nontrivial example: $R = \{0, 1, 2\}$ with birth–death generator

$$K = \begin{pmatrix} -u_0 & u_0 & 0 \\ d_1 & -(u_1 + d_1) & u_1 \\ 0 & d_2 & -d_2 \end{pmatrix}, \qquad u_0 = d_2 = 1, \quad u_1 = d_1 = 2. \tag{25}$$

The stationary distribution is $\mu = (d_1 d_2,\ u_0 d_2,\ u_0 u_1)/(d_1 d_2 + u_0 d_2 + u_0 u_1) = (2/5, 1/5, 2/5)$. The zero-mean subspace V_0 is two-dimensional, and the eigenvalues of $-K$ on V_0 are $\{1, 5\}$, so the spectral gap is $\gamma = 1$ and a faster eigenmode at rate 5 also exists.

Failure-mode response (un-centered). As a first nonlinear response, take the qubit depolarising perturbation

$$\mathcal{N}_r[\rho] \ = \ \alpha_r(\tfrac{\mathbf{1}}{2} - \rho), \qquad \alpha = (+1, -3, +1), \tag{26}$$

so that $\sum_r \mu_r \alpha_r = \frac{2}{5}(1) + \frac{1}{5}(-3) + \frac{2}{5}(1) = \frac{1}{5} \neq 0$. This $\mathcal{N}$ is *not* zero-mean and does not satisfy the centering condition derived from assumption (A3): it represents a persistent nonlinear anomaly that cannot be absorbed by the Markov erasure, and is displayed in Figure 1 as the dashed curve that settles to $|\sum_r \mu_r \alpha_r| = 1/5$ rather than decaying.

Centered slow-mode response. For an illustration of the gap-controlled decay, choose the centered observable

$$\tilde{\alpha} \ = \ (-1,\ 0,\ +1), \qquad \sum_r \mu_r \tilde{\alpha}_r = -\tfrac{2}{5} + 0 + \tfrac{2}{5} = 0, \tag{27}$$

which is centered by construction and is, up to normalization, the right eigenvector of K at eigenvalue $\lambda = -1$ (the slow mode realizing the spectral gap). The Drazin inverse K^D gives

$$G_r \ = \ (K^D \tilde{N})_r, \qquad \tilde{\mathcal{N}}_r = \tilde{\alpha}_r(\tfrac{\mathbf{1}}{2} - \rho), \tag{28}$$

computed explicitly via (24) (gauge $G_0 = 0$): $J_0 = \mu_0 \tilde{\alpha}_0 = \frac{2}{5}(-1) = -\frac{2}{5}$; $J_1 = J_0 + \mu_1 \tilde{\alpha}_1 = -\frac{2}{5} + 0 = -\frac{2}{5}$; hence $G_1 = J_0/(\mu_0 u_0) = -1$ and $G_2 = G_1 + J_1/(\mu_1 u_1) = -2$. The zero-mean Drazin form is

$G = (+1, 0, -1)$ (related to $(0, -1, -2)$ by subtracting the constant $\bar{G}_\mu = -1$); both satisfy $KG = \tilde{N}$, as verified to machine precision by `three_state_example.py`.

Decay envelope. Let $\omega_t = e^{tK}\nu_0$ be the record distribution starting from a non-stationary initial $\nu_0 = (1, 0, 0)$. The Cheeger conductance of the chain (25) is $\Phi_K = \min_{S:\mu(S)\le 1/2} \frac{\mu_0 u_0}{\mu_0} = 1$ (the edge-$0 \to 1$ bottleneck), giving $\gamma \ge 1/2$ by Lemma 2. The exact gap is $\gamma = 1$ (Cheeger bound conservative by a factor of 2). Because $\tilde{\alpha} = (-1, 0, 1)$ has been chosen on the slow eigenmode, the residual $e_t := |\sum_r \omega_t(r)\tilde{\alpha}_r|$ decays at exactly the gap rate $\gamma = 1$ rather than at a faster eigenrate; the numerical fit in `three_state_example.py` returns slope -1.0000 to four digits. An observable concentrated on the fast mode $\lambda = -5$ would decay at rate 5 instead — the gap is a *lower bound* on the decay rate of arbitrary centered observables, not the actual rate of every such observable.

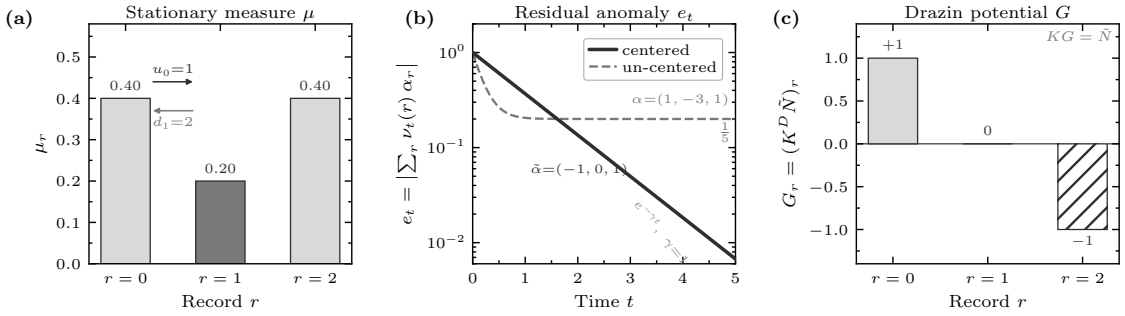

Figure 1: *Minimal finite-record illustration of the CPE mechanism.* Generator (25): K with rates $u_0 = d_2 = 1$, $u_1 = d_1 = 2$; stationary measure $\mu = (2/5, 1/5, 2/5)$; spectrum $\mathrm{spec}(-K|_{V_0}) = \{1, 5\}$, so spectral gap $\gamma = 1$. *Left:* stationary weights μ_r. *Middle:* residual anomaly $e_t = |\sum_r \nu_t(r)\alpha_r|$ vs. time from $\nu_0 = (1, 0, 0)$. Centered slow-mode observable $\tilde{\alpha} = (-1, 0, +1)$ (solid blue) decays at gap rate $\gamma = 1$, matching e^{-t} (dotted). Un-centered $\alpha = (+1, -3, +1)$ (dashed red) does not decay; it settles to $|\sum_r \mu_r\alpha_r| = 1/5$, the persistent Ward anomaly of Theorem 1. *Right:* Drazin potential $G = K^D\tilde{N}$, satisfying $KG = \tilde{N}$ to machine precision. Generated by `numerics/three_state_example.py`.

Code simulation (Appendix D). A companion operator-algebra code simulation (`numerics/tensor_network_c`) demonstrates the same mechanism in the code setting of App. B, including verification of $K^{\mathrm{code}}G = \tilde{\mathcal{N}}$ and the expectation-value CPTP approximation of App. B.6; details and figure are deferred to App. D.

4 General CPE closure theorem

Let Φ_t^0 be the ordinary linear channel induced by the zero-order local dynamics — i.e., the channel one would have written down ignoring the nonlinear response. Let $\bar{\omega}_t^{(\lambda)}$ denote the record-averaged state at cutoff λ, evolved under the full (nonlinear, record-coupled) dynamics with the small coupling ε.

4.1 Statement of the closure theorem

Theorem 2 (Conditional CPE closure at finite regulator)**.** *This theorem is an abstract bookkeeping result: it states that* if *a finite record system $\mathfrak{D}_\lambda$ satisfies the following five model assumptions* (A1)–

(A5), then *the error bound* (30) *holds. The theorem makes no claim about which regulators satisfy these assumptions; that burden is carried by the model-specific arguments in §5 and Appendices A–C.*

Assume that the model supplies a finite record system $\mathfrak{D}_\lambda$ *satisfying:*

(A1) ***Projective tightness:*** *for every local observable* A*, continuum coarse-graining errors obey* $\eta_A(\lambda) \to 0$ *as* $\lambda \to 0$*.*

(A2) ***Uniform erasure resolvent:*** *on zero-mean records,*

$$\left\| e^{t\widehat{K}_\lambda} P_{0,\lambda} \right\| \le M_R e^{-\gamma_R t} \tag{29}$$

with M_R, γ_R *independent of* λ *after the chosen renormalization.*

(A3) ***Stationary anomaly cancellation:*** $a_\lambda := \sup_\omega \|\Pi_{\mu_\lambda} \mathcal{N}_\lambda[\omega]\| \to 0$*.*

(A4) ***Transport-exactness:*** $\dot{\mathcal{G}}_\lambda = \widehat{K}_\lambda \mathcal{H}_\lambda + B_\lambda$ *along the zero-order flow, with* $b_\lambda(T) := \sup_{t \le T} \|B_\lambda[\omega_t^0]\| \to 0$*.*

(A5) ***Bounded causal contraction:*** $Q_\lambda h_\lambda + h_\lambda Q_\lambda = P_{0,\lambda}$ *with* $\sup_\lambda \|h_\lambda\|_{\mathrm{ren}} < \infty$*, and the filtered Maurer–Cartan expansion lies inside its convergence radius (Definition 3 below).*

Then for finite T *and any bounded local observable* A*,*

$$\sup_{0 \le t \le T} \left| \bar{\omega}_t^{(\lambda)}(A) - \Phi_t^0(\bar{\omega}_0)(A) \right| \le \eta_A(\lambda) \|A\| + C_A \varepsilon \left[a_\lambda T + b_\lambda(T) T + \delta_{\mathrm{rec}}^{(1)}(T, \lambda) \right] + O(\varepsilon^2), \tag{30}$$

where $\delta_{\mathrm{rec}}^{(1)}$ *is the initial/final record disequilibrium boundary term defined in* (42) *below. If all residuals vanish and the higher-order Maurer–Cartan series converges, the record-erased dynamics converges to* Φ_t^0*.*

4.2 Filtered Maurer–Cartan expansion

Condition (e) of Theorem 2 requires a precise definition of the convergence radius of the foliation-curvature series.

Definition 3 (Filtered Maurer–Cartan expansion)**.** Let $V_0 \otimes \mathcal{X}$ be the Banach space of zero-mean $\mathcal{X}$-valued cochains at cutoff λ, equipped with norm $\|\cdot\|$. Let $X_\lambda = \sum_{n \ge 1} \varepsilon^n X_{n,\lambda}$ be a formal power series in ε with coefficients $X_{n,\lambda} \in V_0 \otimes \mathcal{X}$, and let h_λ be the contracting homotopy of condition (e). Define the *filtered norm*

$$\|X_\lambda\|_{\mathrm{filt}} := \sum_{n \ge 1} \varepsilon^n \, \|X_{n,\lambda}\| \,. \tag{31}$$

The Maurer–Cartan equation

$$Q_\lambda X_\lambda + \tfrac{1}{2}[X_\lambda, X_\lambda] = 0 \tag{32}$$

is said to *converge in the filtered norm* if the recursive solution

$$X_{n,\lambda} = -\tfrac{1}{2} \, h_\lambda \sum_{p+q=n} [X_{p,\lambda}, X_{q,\lambda}], \qquad n \ge 2, \tag{33}$$

generated from a given first-order term $X_{1,\lambda} = \mathcal{G}_\lambda$ satisfies $\|X_\lambda\|_{\mathrm{filt}} < \infty$.

Proposition 1 (Convergence criterion for the filtered MC expansion)**.** *Let* $C_h := \sup_\lambda \|h_\lambda\|_{\mathrm{ren}} < \infty$ *and* $C_{[\cdot,\cdot]} < \infty$ *a constant such that* $\|[X,Y]\| \le C_{[\cdot,\cdot]}\,\|X\|\,\|Y\|$ *for all* $X, Y \in V_0 \otimes \mathcal{X}$*. If* $\varepsilon\, C_h\, C_{[\cdot,\cdot]}\, \|X_{1,\lambda}\| < \frac{1}{4}$*, then the recursion* (33) *converges in the filtered norm and*

$$\|X_\lambda\|_{\mathrm{filt}} \;\le\; \frac{1 - \sqrt{1 - 4\varepsilon C_h C_{[\cdot,\cdot]}\,\|X_{1,\lambda}\|}}{2\, C_h\, C_{[\cdot,\cdot]}}. \tag{34}$$

Proof. Let $\sigma_n = \|X_{n,\lambda}\|$. From (33) and the algebra property of the bracket,

$$\sigma_n \;\le\; \tfrac{1}{2}\, C_h\, C_{[\cdot,\cdot]} \sum_{p+q=n} \sigma_p \sigma_q, \qquad n \ge 2, \tag{35}$$

with $\sigma_1 = \|X_{1,\lambda}\|$. This is the standard Cauchy-product inequality governing the coefficients of the generating function $\sigma(z) := \sum_{n\ge 1} \sigma_n z^n$:

$$\sigma(z) \;\le\; \sigma_1 z + \tfrac{1}{2}\, C_h\, C_{[\cdot,\cdot]}\, \sigma(z)^2. \tag{36}$$

Solving the quadratic for $\sigma(z)$ gives (34) at $z = \varepsilon$, valid when the discriminant is nonnegative, i.e., when $\varepsilon C_h C_{[\cdot,\cdot]} \sigma_1 < \frac{1}{4}$. This is the standard homological-perturbation-lemma estimate (cf. [29]). □

Remark 5 (Relation to L_∞ minimal models). The Maurer–Cartan recursion (33) is a special case of the homotopy-transfer construction for L_∞-algebras: given a contracting homotopy on a chain complex, the deformation theory transports to a minimal L_∞ structure on the cohomology. In our setting the contracting homotopy is h_λ from condition (e) and the deformation parameter is the coupling ε. The convergence radius (34) is the radius in which the transported L_∞ structure remains finite-norm; outside that radius the higher L_∞ brackets diverge and the perturbative expansion breaks down. The general theory [29] gives the same radius via a more abstract route. For our purposes the explicit quadratic bound is sufficient because the foliation-curvature problem in each model is treated as a perturbative expansion to a finite order in ε, with the higher orders absorbed into the $O(\varepsilon^2)$ remainder of (30).

4.3 Proof of the closure theorem

Proof of Theorem 2. We decompose the response according to the Poisson lemma (Lemma 1):

$$\mathcal{N}_\lambda = \widehat{K}_\lambda \mathcal{G}_\lambda + \Pi_{\mu_\lambda} \mathcal{N}_\lambda, \tag{37}$$

where $\mathcal{G}_\lambda = \widehat{K}_\lambda^D \mathcal{N}_\lambda$ on the zero-mean part and $\Pi_{\mu_\lambda}\mathcal{N}_\lambda$ is the anomaly.

Step 1: anomaly contribution. The anomaly term contributes a perturbation to the dynamics with magnitude bounded by a_λ uniformly in ω. Over a time interval T, the cumulative effect on a bounded observable A is at most $C_A \varepsilon a_\lambda T$ at first order in ε, by a Duhamel expansion of the perturbed semigroup.

Step 2: coboundary contribution (transport identity in full). The contribution of $\widehat{K}_\lambda \mathcal{G}_\lambda$ to the record-averaged dynamics is

$$\Delta_{\mathrm{cob}}(T) \;:=\; \varepsilon \int_0^T \nu_t(\widehat{K}_\lambda \mathcal{G}_{\lambda,t})\, \mathrm{d}t, \tag{38}$$

where ν_t is the record-side probability distribution at time t evolved under the zero-order Markov semigroup $\dot\nu_t = \nu_t \widehat{K}_\lambda$. Note carefully: the Markov action on the row vector is $\nu_t \widehat{K}_\lambda$, while the action

on column-valued potentials is $\widehat{K}_\lambda \mathcal{G}_{\lambda,t}$, and the pairing satisfies $\nu_t(\widehat{K}_\lambda \mathcal{G}_{\lambda,t}) = (\nu_t \widehat{K}_\lambda)(\mathcal{G}_{\lambda,t}) = \dot{\nu}_t(\mathcal{G}_{\lambda,t})$. This is the key adjoint identity that makes the coboundary into a total derivative. We compute:

$$\begin{aligned} \frac{d}{dt}\big[\nu_t(\mathcal{G}_{\lambda,t})\big] &= \dot{\nu}_t(\mathcal{G}_{\lambda,t}) + \nu_t(\dot{\mathcal{G}}_{\lambda,t}) \\ &= \nu_t(\widehat{K}_\lambda \mathcal{G}_{\lambda,t}) + \nu_t(\dot{\mathcal{G}}_{\lambda,t}). \end{aligned} \tag{39}$$

Integrating from 0 to T,

$$\int_0^T \nu_t(\widehat{K}_\lambda \mathcal{G}_{\lambda,t})\,\mathrm{d}t = \nu_T(\mathcal{G}_{\lambda,T}) - \nu_0(\mathcal{G}_{\lambda,0}) - \int_0^T \nu_t(\dot{\mathcal{G}}_{\lambda,t})\,\mathrm{d}t. \tag{40}$$

This is the *moving-potential identity*: it converts the time integral of a K-coboundary into a boundary term plus an integral of the time-derivative of the potential.

Step 3: transport-exactness applied to the residual integral. By condition (d), $\dot{\mathcal{G}}_{\lambda,t} = \widehat{K}_\lambda \mathcal{H}_{\lambda,t} + B_{\lambda,t}$. Substituting and applying (40) once more to the $\widehat{K}_\lambda \mathcal{H}_\lambda$ term gives

$$\int_0^T \nu_t(\dot{\mathcal{G}}_{\lambda,t})\,\mathrm{d}t = \big[\nu_T(\mathcal{H}_{\lambda,T}) - \nu_0(\mathcal{H}_{\lambda,0})\big] - \int_0^T \nu_t(\dot{\mathcal{H}}_{\lambda,t})\,\mathrm{d}t + \int_0^T \nu_t(B_{\lambda,t})\,\mathrm{d}t. \tag{41}$$

Recursive iteration (if $\mathcal{H}_\lambda$ itself has a transport-exact decomposition) generates further boundary terms, all bounded uniformly in λ by the resolvent bound (29). We collect all boundary contributions into

$$\delta^{(1)}_{\mathrm{rec}}(T,\lambda) := \|\nu_T(\mathcal{G}_{\lambda,T}) - \nu_0(\mathcal{G}_{\lambda,0})\| + \|\nu_T(\mathcal{H}_{\lambda,T}) - \nu_0(\mathcal{H}_{\lambda,0})\| + \cdots, \tag{42}$$

which vanishes when $\nu_0 = \mu_\lambda$ and $\nu_T \to \mu_\lambda$ (record equilibration), because $\mu_\lambda(\mathcal{G}_\lambda) = 0$ by zero-mean. The residual B_λ contributes at most $b_\lambda(T)T$.

Step 4: collecting first-order terms. Summing the anomaly contribution from Step 1 and the coboundary contribution from Steps 2–3,

$$\left|\bar{\omega}^{(\lambda)}_T(A) - \Phi^0_T(\bar{\omega}_0)(A)\right| \le \eta_A(\lambda)\,\|A\| + C_A\varepsilon\big[a_\lambda T + b_\lambda(T)T + \delta^{(1)}_{\mathrm{rec}}(T,\lambda)\big] + O(\varepsilon^2), \tag{43}$$

where $\eta_A(\lambda)\,\|A\|$ comes from projective tightness in condition (a). This is the bound (30) at $t = T$; taking $\sup_{0\le t\le T}$ on the right gives the time-uniform statement.

Step 5: higher-order foliation curvature. At order ε^2 and higher, the local glueings of the response across the causal foliation generate Maurer–Cartan corrections of the form

$$Q_\lambda X_\lambda + \tfrac{1}{2}[X_\lambda, X_\lambda] = 0. \tag{44}$$

By condition (e) and Proposition 1, the recursion $X_{n,\lambda} = -\frac{1}{2}h_\lambda \sum_{p+q=n}[X_{p,\lambda}, X_{q,\lambda}]$ generates a convergent solution provided $\varepsilon C_h C_{[\cdot,\cdot]}\,\|X_{1,\lambda}\| < \frac{1}{4}$, with $\|X_\lambda\|_{\mathrm{filt}}$ bounded by (34). Each higher-order term satisfies its own coboundary identity by virtue of $X_{n,\lambda} \in V_0 \otimes \mathcal{X}$ (acyclicity in degree ≥ 1) and is absorbed into the $O(\varepsilon^2)$ remainder in (30). □

The remaining sections show how the abstract symbols in Theorem 2 are realized in four explicit regulators.

5 Worked model I: JT gravity with Schwarzian edge records

5.1 Microscopic setup

The Euclidean JT action with matter has the schematic form

$$I_{\rm JT} = -\frac{1}{16\pi G}\int_M \sqrt{g}\,\Phi\left(R+\frac{2}{L^2}\right) - \frac{1}{8\pi G}\int_{\partial M}\Phi_b K + I_{\rm m}[g,\psi] + I_{\rm ct}. \tag{45}$$

With nearly-AdS_2 boundary conditions, the low-energy boundary mode is a reparametrization $f(u)$ governed by the Schwarzian action

$$I_{\rm Sch} = -C\int {\rm d}u\,\left\{\tan\frac{\pi f(u)}{\beta}, u\right\}, \qquad C = \frac{\Phi_r}{8\pi G}. \tag{46}$$

This is the standard nearly-AdS_2/JT boundary dynamics described by Maldacena, Stanford, and Yang [8]. The Schwarzian energy is

$$E_f = C\left\{\tan\frac{\pi f}{\beta}, u\right\}, \tag{47}$$

up to the conventional sign choice for Euclidean continuation. The horizon-dilaton variable Φ_h is fixed by the JT black-hole solution and is a monotone function of energy; in the semiclassical normalization one may write

$$S_{\rm BH} = S_0 + \frac{\Phi_h}{4G}, \qquad E = \frac{\Phi_h^2}{16\pi G\Phi_r L} + O(\lambda_{\rm ct}), \tag{48}$$

where the precise coefficient depends on the chosen boundary convention. Only monotonicity and smoothness are used below.

5.2 Record algebra

Fix a UV/IR regulator $\lambda = (\Delta E, \Delta\Phi, E_{\max}, \Phi_{\max})$. Partition the allowed Schwarzian energy interval into bins $I_i = [E_i, E_i + \Delta E)$ and the horizon dilaton interval into bins $J_j = [\Phi_j, \Phi_j + \Delta\Phi)$. Allow a finite set M_k of coarse matter-shock histories, e.g. k labels the total injected null energy in a time cell. The record set is

$$R_\lambda^{\rm JT} = \{r = (i,j,k) : E \in I_i,\ \Phi_h(E) \in J_j,\ \text{matter record } M_k\}. \tag{49}$$

The abelian record algebra is

$$\mathfrak{Z}_\lambda^{\rm JT} = \ell^\infty(R_\lambda^{\rm JT}) = {\rm span}\{Z_{ijk}\}, \qquad Z_{ijk}Z_{i'j'k'} = \delta_{ii'}\delta_{jj'}\delta_{kk'}Z_{ijk}. \tag{50}$$

It is not the center of a type-III local algebra. It is a finite split-boundary register for the regulated gravitational boundary mode.

5.3 Why preparation changes the record

A matter insertion changes the boundary energy through the gravitational constraint. In Lorentzian signature the reparametrization mode satisfies an energy-balance equation of the form

$$\frac{{\rm d}E_f(u)}{{\rm d}u} = \mathcal{F}_{\rm in}(u) - \mathcal{F}_{\rm out}(u) + O(\lambda_{\rm grav}), \tag{51}$$

where $\mathcal{F}_{\rm in/out}$ are matter fluxes across the regulated boundary or horizon. Integrating over a preparation interval $[u_0, u_1]$ gives

$$\Delta E_f = \int_{u_0}^{u_1} (\mathcal{F}_{\rm in} - \mathcal{F}_{\rm out}) \mathrm{d}u + O(\lambda_{\rm grav}). \tag{52}$$

Because Φ_h is a function of E_f, any uncompensated preparation changing energy also changes the bin (i, j) once the shift exceeds the coarse-graining scale. This is the JT version of the CPE record principle: the record is forced by the gravitational boundary constraint rather than by an external measuring pointer.

5.4 Erasure generator

The Schwarzian boundary mode coupled to a large matter sector or to an auxiliary bath has a unitary total dynamics. In a van Hove/Davies scaling of weak coupling, the reduced dynamics of the finite energy bins becomes Markovian [30].

Remark 6 (Status of the Markov rates: input vs. derivation). The birth–death rates u_i, d_i below are an *input* to the JT-record model, not a derivation from JT gravity itself. The Davies/van Hove construction guarantees that *some* Markovian reduction exists in the weak-coupling limit, with rates determined by Fermi's golden rule between adjacent energy bins. But the explicit rates depend on (i) the choice of bath, (ii) the choice of system–bath coupling, and (iii) the precise van-Hove scaling, none of which is fixed by JT gravity alone. We therefore treat (u_i, d_i) as the data of the erasure model, subject only to the requirements: (a) primitivity (the rate graph is connected), (b) the detailed-balance choice (58) relative to the Schwarzian thermal distribution (57), and (c) uniformity of the Cheeger gap across the family of cutoffs. Different physically motivated coupling choices (e.g., a 1D thermal bath, a coupling to bulk matter quanta, a coupling to a UV-cutoff regulator) give different specific rates but all satisfy (a)–(c). Establishing (a)–(c) for a specific JT coupling is the model-building step that is *not* done in this paper.

For adjacent energy bins, define a birth-death generator

$$\begin{aligned} K_{i,i+1} &= u_i = \Gamma_i^+, & K_{i,i-1} &= d_i = \Gamma_i^-, \\ K_{ii} &= -(u_i + d_i), \end{aligned} \tag{53}$$

with missing boundary rates set to zero.

Microscopic origin of the rates. A concrete (and not unique) microscopic realisation of (u_i, d_i) proceeds as follows. Couple the Schwarzian boundary mode to a bosonic bath via a linear coupling

$$H_{\rm tot} \;=\; H_{\rm Sch} \;+\; \sum_q \omega_q \, b_q^\dagger b_q \;+\; \sqrt{\varepsilon}\, \hat{\mathcal{O}}_{\rm Sch} \otimes \sum_q g_q (b_q + b_q^\dagger), \tag{54}$$

where $\hat{\mathcal{O}}_{\rm Sch}$ is a bin-changing boundary operator (e.g., a smeared Schwarzian energy density) and $\{g_q\}$, $\{\omega_q\}$ define a bath spectral density $J(\omega) = \sum_q |g_q|^2 \delta(\omega - \omega_q)$. In the van Hove / weak-coupling scaling ($\varepsilon \to 0$, $t \to t/\varepsilon^2$) the Davies map [30] reduces the bin-marginal dynamics to a Markov chain with rates given by Fermi's golden rule:

$$u_i \;=\; 2\pi \, J(\omega_{i,i+1}) (1 + n_B(\omega_{i,i+1})) \, |\langle i+1 | \hat{\mathcal{O}}_{\rm Sch} | i \rangle|^2, \tag{55}$$

$$d_i \;=\; 2\pi \, J(\omega_{i,i-1}) \, n_B(\omega_{i,i-1}) \, |\langle i-1 | \hat{\mathcal{O}}_{\rm Sch} | i \rangle|^2, \tag{56}$$

where $\omega_{i,j} = (E_i - E_j)/\hbar$, $n_B(\omega) = (e^{\beta\omega} - 1)^{-1}$ is the Bose distribution at the bath temperature β^{-1}, and the matrix elements $\langle i \pm 1|\hat{\mathcal{O}}_{\rm Sch}|i\rangle$ are bin-overlap integrals controlled by the Schwarzian density of states (57). Detailed balance (58) then follows from the KMS condition $J(\omega)n_B(\omega) = J(-\omega)(1 + n_B(-\omega))$ for a thermal bath at the same temperature. Primitivity (connectivity of the rate graph) is automatic for any bath with continuous spectrum overlapping all bin gaps.

We emphasise that the choice of bath spectrum $J(\omega)$ and of the bin-changing operator $\hat{\mathcal{O}}_{\rm Sch}$ are model inputs not fixed by JT gravity alone (Remark 6); equation (54) is one canonical choice that produces a closed-form birth–death structure. Alternative microscopic realisations (e.g., coupling to bulk matter, dilaton fluctuations, or a UV-cutoff regulator) yield qualitatively similar rate structures. What *is* model-independent is the asymptotic stationary distribution (57) and the existence of a uniform spectral gap, both of which are required for closure assumption (A2). A thermal Schwarzian stationary distribution may be written

$$\mu_i = \frac{1}{Z_\lambda}\rho_{\rm Sch}(E_i)e^{-\beta E_i}\Delta E, \qquad \rho_{\rm Sch}(E) \propto \sinh\left(2\pi\sqrt{2CE}\right), \tag{57}$$

where the density is the standard Schwarzian density of states. The detailed-balance choice

$$\mu_i u_i = \mu_{i+1} d_{i+1} \tag{58}$$

is sufficient, not necessary. More generally, any connected finite rate graph with stationary distribution (57) is primitive. On the zero-mean subspace,

$$\left\|e^{tK}P_0\right\|_{L^2(\mu)} \le e^{-\gamma_{\rm JT}t}, \qquad \gamma_{\rm JT} \ge \frac{1}{2}\Phi_K^2, \tag{59}$$

where Φ_K is the conductance of the finite chain. Equation (59) supplies the required resolvent bound $\left\|K^D P_0\right\| \le 1/\gamma_{\rm JT}$.

5.5 Stationary Ward anomaly and Poisson solution

The centering condition $\Pi_\mu \mathcal{N} = 0$ in the JT model is forced — on a restricted but explicitly identifiable subspace of responses — by the SL(2,$\mathbb{R}$) Ward identity of the Schwarzian partition function. We isolate the domain on which the Ward identity applies, defer the identity-primary exclusion to an explicitly named domain assumption (A3′), and state the conclusion as a Proposition. This phrasing is preferred to the older form "the Ward identity derives $\Pi_\mu \mathcal{N} = 0$ for any physically realized response," which conflated a Ward-identity statement about non-identity primaries with an additional physical input about the absence of state-dependent identity-sector counterterms.

Step 1: SL(2,$\mathbb{R}$) symmetry of the Schwarzian. The Schwarzian action (46) is invariant under the Möbius (SL(2,$\mathbb{R}$)) action

$$\tan\frac{\pi f(u)}{\beta} \longmapsto \frac{a\,\tan\frac{\pi f(u)}{\beta} + b}{c\,\tan\frac{\pi f(u)}{\beta} + d}, \qquad ad - bc = 1. \tag{60}$$

Equivalently, the Schwarzian derivative vanishes on Möbius transformations. The associated conserved Noether currents generate a triplet of zero modes which, in the thermal ensemble at inverse temperature β, are exactly compensated by the Faddeev–Popov measure of the localization

computation of Stanford and Witten [9]. As a consequence, the Schwarzian one-point function of any reparametrization-covariant insertion $\mathcal{O}[f]$ satisfies

$$\Big\langle \sum_{i=1}^{3} \delta_{\xi_i} \mathcal{O}[f] \Big\rangle_\beta \;=\; 0, \tag{61}$$

where $\{\xi_i\}_{i=1}^3$ is a basis of the SL(2,$\mathbb{R}$) generators acting on f.

Step 2: from the Ward identity to the response structure. A local matter preparation in the JT background corresponds, in the boundary description, to insertion of a Schwarzian-covariant vertex operator $V[f]$ at the regulated boundary. By the gravitational constraint (51), the response of such an insertion to a small nonlinear coupling ε takes the form

$$\mathcal{N}[f,\omega] \;=\; \sum_a c_a(\omega)\, \mathcal{O}_a[f] \;+\; \xi \cdot V[f] \cdot \omega, \tag{62}$$

where $\mathcal{O}_a[f]$ are SL(2,$\mathbb{R}$)-covariant primaries built from f and its derivatives, and $\xi \cdot V[f]$ denotes the action of an SL(2,$\mathbb{R}$) generator on V. The first term is the genuine state-dependent response; the second term is a gauge artifact of the SL(2,$\mathbb{R}$) zero-mode integration. Applying the Ward identity (61) to the Schwarzian thermal expectation value yields

$$\sum_i \mu_i \, \langle \mathcal{O}_a[f] \rangle_{\beta, E_i} \;=\; \langle \mathcal{O}_a[f] \rangle_\beta \;=\; 0 \quad \text{for } \mathcal{O}_a[f] \text{ a non-identity SL(2,}\mathbb{R}\text{)-primary,} \tag{63}$$

because non-identity primaries have vanishing thermal one-point function by SL(2,$\mathbb{R}$) covariance (their one-point functions transform nontrivially under the residual Möbius group of the thermal disk, and the only invariant one-point function is a constant, which must be zero for a non-identity primary).

Schwarzian-covariant primaries: what (63) actually constrains. The strength of the Ward identity depends critically on which subspace of $\mathcal{N}[\omega]$ falls in the non-identity primary representation. We make this precise.

A *Schwarzian-covariant primary of weight h* is, by definition, a local functional $\mathcal{O}[f](u)$ that transforms under the Möbius action (60) as

$$\mathcal{O}[\tilde{f}](u) \;=\; (\tilde{f}'(u))^{-h}\, \mathcal{O}[f](\tilde{f}(u)), \tag{64}$$

where $\tilde{f}$ is the Möbius-transformed reparametrization [8]. By the Stanford–Witten localization [9], the Schwarzian thermal one-point function of a primary of weight $h \geq 1$ vanishes:

$$\langle \mathcal{O}[f] \rangle_\beta \;=\; 0 \qquad \text{for any non-identity primary with } h \geq 1. \tag{65}$$

This is (63) stated with its precise domain.

Which nonlinear responses lie in this subspace? The nonlinear response $\mathcal{N}_i[\omega]$ in the JT regulator is constructed by inserting a local boundary deformation $\varepsilon\, V[f] \cdot \omega$ that depends on the boundary state ω and the regulated reparametrization profile $f(u)$. Up to a choice of regulator, $V[f]$ is a local functional of f and its first k derivatives (k fixed by the order of the nonlinearity). Such functionals admit a unique decomposition into Schwarzian covariant primaries plus descendants [8] §3. The descendant part is Möbius-trivial (it is a derivative of a lower-weight primary) and contributes

only to the gauge artifact $\xi \cdot V[f]$ of (62), not to the physical response $\mathcal{N}^{\perp}$. Therefore the physical state-dependent component $\mathcal{N}^{\perp}$ lies in the direct sum of primary representations $\bigoplus_{h\geq 1} \mathcal{R}_h$, and (63) applies to it directly.

The only piece *not* controlled by (65) is the weight-zero (identity-primary) contribution: a state-dependent constant $a(\omega)$ that does not depend on f at all. This is what the next paragraph rules out at the level of the Schwarzian path integral.

Why the identity-primary anomaly is excluded. A nonzero identity-primary contribution $a(\omega)\mathcal{V}$ would correspond to a state-dependent shift of the Schwarzian effective action by a constant counterterm. In the Stanford–Witten localization [9], this shift is fixed by two independent requirements:

(i) *Background independence of the Schwarzian path integral.* The partition function $Z_\beta = \int [\mathcal{D}f]\, e^{-S_{\rm Sch}[f]}$ is computed by one-loop exact localization onto Möbius orbits, with the Faddeev–Popov measure fixed by SL(2,$\mathbb{R}$) gauge invariance. A state-dependent identity-primary shift $a(\omega)$ would multiply Z_β by a state-dependent overall constant $e^{-\varepsilon\, a(\omega)}$, violating the universal $\beta^{3/2} e^{C/\beta}$ scaling derived from the localization measure.

(ii) *Consistency with the matter sector decoupling at leading order in G_N.* At leading order, the Schwarzian sector and the matter sector factorise: $Z_{\rm tot} = Z_{\rm Sch} \cdot Z_{\rm matter}[\omega]$. An identity-primary contribution to $\mathcal{N}$ would re-couple the two sectors through a state-dependent $a(\omega)$, contradicting the leading-order factorisation that defines the JT regulator.

Both requirements are physical inputs at the level of the regulator construction, not consequences of the dynamical equations. When they hold, the identity-primary contribution $a(\omega)$ vanishes, and consequently $\mathcal{N}^{\perp} \in \bigoplus_{h\geq 1} \mathcal{R}_h$. We *adopt this exclusion as a domain assumption* on the JT regulator's nonlinear responses (assumption (A3′) below); it is the physical content of "no state-dependent identity-sector counterterm."

Caveat (open question). If the JT regulator is modified to include matter back-reaction at order G_N or higher, the factorisation in (ii) breaks down and an identity-primary contribution could re-emerge as a back-reaction counterterm. Whether the closure mechanism survives such a modification is a model-dependent question we do not address here; see Open Problem (v) in §8.

Step 3: the domain-restricted Proposition. With Steps 1–2 in hand we can isolate the precise mathematical content of the centering claim from the physical input that controls the identity sector.

Definition 4 (The Schwarzian non-identity domain $\mathcal{D}_{\rm JT}$)**.** Let $\mathcal{D}_{\rm JT}$ denote the subspace of bin-indexed nonlinear responses $\mathcal{N} = \{\mathcal{N}_i[\omega]\}$ such that the state-dependent part of each $\mathcal{N}_i[\omega]$ is constructed from local Schwarzian functionals $V[f]$ whose primary decomposition contains no weight-zero (identity) component:

$$\mathcal{N}_i[\omega] \;=\; \sum_{h\geq 1} \mathcal{O}_{i,h}[f] \cdot \mathcal{V}_h[\omega] \;+\; (\text{SL(2,}\mathbb{R}\text{) descendants}), \tag{66}$$

where each $\mathcal{O}_{i,h}$ is a Schwarzian primary of weight $h \geq 1$ in the sense of (64). Descendants are Möbius-trivial and contribute only to the gauge artifact term $\xi \cdot V[f]$ of (62).

Proposition 2 (Schwarzian centering on $\mathcal{D}_{\rm JT}$)**.** *Let K be the Schwarzian birth–death generator of §5.4 with stationary distribution μ given by (57). For every $\mathcal{N} \in \mathcal{D}_{\rm JT}$,*

$$\Pi_\mu \mathcal{N} \;:=\; \sum_i \mu_i \, \mathcal{N}_i[\omega] \;=\; 0 \qquad \textit{for all states } \omega. \tag{67}$$

Proof. Fix ω and write $\mathcal{N}_i[\omega] = \sum_{h\geq 1} \mathcal{O}_{i,h}[f]\, \mathcal{V}_h[\omega]$ modulo descendants. Each $\mathcal{O}_{i,h}$ is a non-identity Schwarzian primary of weight $h \geq 1$. The Stanford–Witten localization [9] gives (65): $\langle \mathcal{O}_{i,h}[f] \rangle_\beta = 0$ for each $h \geq 1$, with the bin index i playing the role of the Cartan label $L_0 - \bar{E}_\mu$ (which is itself centered as in (68) below). Summing $\mu_i \langle \mathcal{O}_{i,h} \rangle_\beta$ over i at fixed h gives zero on each isotypic component, and hence on the full sum. The descendant piece contributes only to the gauge artifact, which is annihilated by the SL(2,$\mathbb{R}$) projector Π_μ acting through the localization measure. □

Assumption A3′ (domain restriction, JT instantiation): *The physical nonlinear response of the JT regulator is taken to lie in $\mathcal{D}_{\rm JT}$.* In words: no state-dependent zero-mode counterterm $a(\omega)\mathcal{V}$ in the Schwarzian effective action. This is the JT-specific instantiation of the abstract centering assumption (A1) in the language of §2.4; the two requirements (i) localization-measure background independence and (ii) leading-order matter–Schwarzian factorisation, both stated in the preceding paragraph, are physical defenses of A3′ at order G_N^0.

Scope of Proposition 2. Four points deserve explicit statement:

(1) *Which $\mathcal{N}_i[\omega]$ are Schwarzian primaries?* Those whose insertion operator $\mathcal{O}_{i,h}[f]$ transforms as (64) with $h \geq 1$. This is a checkable algebraic property of a candidate insertion, not a generic property of every functional of f.

(2) *Bin-labelled centered functions that are not Schwarzian primaries.* A function on the energy bins that happens to satisfy $\sum_i \mu_i f_i = 0$ but is not built from a non-identity Schwarzian primary is *not* controlled by Proposition 2. Such functions lie outside $\mathcal{D}_{\rm JT}$; their centering must be verified by direct computation, not inferred from the Ward identity.

(3) *State-dependent identity-sector contamination.* An identity-primary component $a(\omega)\mathcal{V}$ is not excluded by the Ward identity itself, which is a statement about non-identity primaries. Exclusion comes from A3′, defended in (i)–(ii) of the preceding paragraph by background independence of the localization measure and leading-order factorisation. Failure of A3′ (e.g., from G_N back-reaction) returns one to the unconstrained no-go scenario of Theorem 1.

(4) *Zero-mode counterterm.* The phrase "consistent localization measure forbids a state-dependent zero-mode counterterm" is a physical defense of A3′, not a derivation independent of it: the localization measure is a regulator input, and "consistent" means consistent with the two requirements stated above. In a different regulator (e.g., a quantum-extremal-surface refinement at order G_N) the requirements and hence A3′ may need to be reformulated.

Centered response decomposition (in-domain). For $\mathcal{N} \in \mathcal{D}_{\rm JT}$, the energy E_i and the horizon dilaton Φ_i play the role of the (centered) Cartan charges $L_0 - \bar{E}_\mu$ and $\Phi_0 - \bar{\Phi}_\mu$ of SL(2,$\mathbb{R}$), and their thermal centering

$$\sum_i \mu_i (E_i - \bar{E}_\mu) = 0, \qquad \sum_i \mu_i (\Phi_i - \bar{\Phi}_\mu) = 0 \tag{68}$$

is automatic from the definition of $\bar{E}_\mu, \bar{\Phi}_\mu$. The most general SL(2,$\mathbb{R}$)-covariant response in $\mathcal{D}_{\mathrm{JT}}$ built from the bin labels is

$$\mathcal{N}_i[\omega] = \alpha(E_i - \bar{E}_\mu)\mathcal{V}[\omega] + \beta(\Phi_i - \bar{\Phi}_\mu)\mathcal{W}[\omega] + \mathcal{N}_i^{\perp}[\omega], \tag{69}$$

where

$$\bar{E}_\mu = \sum_i \mu_i E_i, \qquad \bar{\Phi}_\mu = \sum_i \mu_i \Phi_i, \qquad \sum_i \mu_i \mathcal{N}_i^{\perp} = 0, \tag{70}$$

the last by Proposition 2 applied to the non-identity primary content of $\mathcal{N}^{\perp}$. Therefore

$$\Pi_\mu \mathcal{N} \;=\; \sum_i \mu_i \mathcal{N}_i \;=\; 0 \qquad \text{for } \mathcal{N} \in \mathcal{D}_{\mathrm{JT}}, \tag{71}$$

which is the closure condition (4) restricted to the domain $\mathcal{D}_{\mathrm{JT}}$ in which the Ward identity applies, modulo the domain assumption A3′ that the JT regulator's physical responses lie in $\mathcal{D}_{\mathrm{JT}}$.

Failure mode. The derivation fails precisely if $\mathcal{N} \notin \mathcal{D}_{\mathrm{JT}}$, i.e., if $\mathcal{N}$ contains an identity-primary piece $a(\omega)\mathcal{V}$ that is constant in i. Then $\Pi_\mu \mathcal{N} = a(\omega)\mathcal{V} \neq 0$ and CPE fails by Theorem 1. In Schwarzian language this is an anomalous shift of the effective action by a state-dependent zero-mode counterterm; in the language of A3′ above, it is precisely the configuration excluded by the JT regulator's localization measure. Whether the next generation of refinements (back-reacted JT, JT with bulk matter at $O(G_N)$, etc.) preserve A3′ is the natural follow-up question stated as Open Problem (v).

Explicit Poisson solution. By Lemma 1, $\Pi_\mu \mathcal{N} = 0$ implies the existence of $\mathcal{G}$ with $\mathcal{N} = K\mathcal{G}$. For the one-dimensional energy chain, the closed-form solution (24) gives

$$\mathcal{G}_i = \sum_{q=0}^{i-1} \frac{1}{\mu_q u_q} \sum_{j=0}^{q} \mu_j \mathcal{N}_j. \tag{72}$$

This is the model-level coboundary potential.

5.6 Transport defect

Along the unperturbed Schwarzian thermal flow, E_i and Φ_i are stationary labels and $\dot{\mathcal{G}} = 0$, so (6) holds with $B = 0$ for a time-independent thermal regulator. If the boundary temperature or cutoff is slowly varied, $\mu = \mu(u)$ and

$$\dot{\mathcal{G}} = \frac{\partial \mathcal{G}}{\partial \beta}\dot{\beta} + \frac{\partial \mathcal{G}}{\partial \lambda}\dot{\lambda}. \tag{73}$$

Since K^D is bounded by (59), the defect obeys

$$\|B(u)\| \leq C\left(\left|\dot{\beta}(u)\right| + \left|\dot{\lambda}(u)\right|\right) \tag{74}$$

for smooth adiabatic variations. Hence $B \to 0$ in the static or adiabatic limit.

5.7 Causal cohomology: two-row bicomplex from the Koszul resolution

The cohomology condition required by Theorem 2(e) is verified for the JT regulator by combining the two-term Koszul resolution of Lemma 3 with a Čech good cover of the JT boundary. The argument is uniform across all four worked regulators (cf. Remark 4); the present subsection records the JT instantiation.

The good cover of the JT boundary. The JT boundary is a one-dimensional Lorentzian time interval $\mathcal{I} = [u_0, u_1]$ (or a circle in the thermal case). Choose a finite open good cover $\mathcal{U} = \{U_\alpha\}_{\alpha=0}^{N}$ of $\mathcal{I}$ by intervals such that every nonempty intersection $U_{\alpha_0 \cdots \alpha_p}$ is again an interval, hence contractible; such a cover always exists for a one-manifold, with bounded nerve multiplicity $C_{\mathrm{cov}}^{\mathrm{JT}} \le 2$ for the standard arrangement of overlapping intervals. This instantiates assumption (A4′) for the JT model.

The Čech contracting homotopy $s : \check{C}^p(\mathcal{U}) \to \check{C}^{p-1}(\mathcal{U})$ is given by the standard partition-of-unity formula

$$(s\,\sigma)_{\alpha_0 \cdots \alpha_{p-1}} \;:=\; \sum_{\alpha} \rho_\alpha \, \sigma_{\alpha \alpha_0 \cdots \alpha_{p-1}}, \qquad \delta s + s \delta = \mathbf{1} - \pi_0, \tag{75}$$

where π_0 is the augmentation projector onto $\check{C}^0$ and $\|s\| \le C_{\mathrm{cov}}^{\mathrm{JT}}$.

The two-row bicomplex. The vertical direction is the two-term Koszul complex of Lemma 3 with $V_0 = V_0^{\mathrm{JT}}$ (the zero-mean subspace of the Schwarzian energy-bin record space) and differential $d = K^{\mathrm{JT}}|_{V_0} : C^0 \to C^1$. The bicomplex relevant to CPE closure is

$$\mathcal{B}^{p,q}(\mathcal{U}; K^{\mathrm{JT}}) \;:=\; \check{C}^p(\mathcal{U}) \;\otimes\; C^q, \qquad p \ge 0, \quad q \in \{0, 1\}, \tag{76}$$

with horizontal differential $\delta : \check{C}^p \to \check{C}^{p+1}$ (Čech coboundary) and vertical differential $d = K^{\mathrm{JT}} : C^0 \to C^1$. The total differential is

$$Q \;:=\; \delta \otimes \mathbf{1}_{C^\bullet} \;+\; (-1)^p \, \mathbf{1}_{\check{C}^\bullet} \otimes d, \tag{77}$$

and $Q^2 = 0$ holds because $\delta^2 = 0$, $d^2 = 0$ vacuously (Lemma 3(i)), and the cross-terms cancel by the Koszul-sign convention. There is no C^q contribution at $q \ge 2$ to track separately — this is the essential simplification.

Acyclicity by Künneth. Both factors of the bicomplex are acyclic on the relevant subspaces:

- $\check{C}^\bullet(\mathcal{U})$: contractible base $\mathcal{I}$ gives $H_\delta^p = 0$ for $p \ge 1$ and $H_\delta^0 = \mathbb{C}$.
- $C^\bullet$: Lemma 3(ii) gives $H^q(C^\bullet) = 0$ for $q \in \{0, 1\}$, with $C^q = 0$ for $q \notin \{0, 1\}$.

By the Künneth theorem for total complexes of bicomplexes,

$$H_Q^n(\mathcal{B}^{\bullet,\bullet}; V_0^{\mathrm{JT}}) \;=\; \bigoplus_{p+q=n} H_\delta^p(\check{C}^\bullet) \otimes H^q(C^\bullet) \;=\; 0 \quad \text{for every } n \ge 0, \tag{78}$$

where the $n = 0$ piece $H_\delta^0 \otimes H^0(C^\bullet) = \mathbb{C} \otimes 0 = 0$ vanishes because $H^0(C^\bullet) = \ker(K|_{V_0}) = 0$. In particular $H_Q^2 = 0$, which instantiates assumption (A5)/(e) of Theorem 2 for the JT model.

Contracting homotopy: existence and norm bound. The total complex $\mathrm{Tot}^\bullet(\mathcal{B}^{\bullet,\bullet})$ is acyclic in degrees ≥ 0 by the Künneth argument above. A contracting homotopy H_{JT} therefore exists. For the quantitative bound needed by Theorem 2(e), we use the Künneth norm estimate of Remark 4: any contracting homotopy built from the Koszul component h (norm $\le 1/\gamma_{\mathrm{JT}}$) and the Čech component s (norm $\le C_{\mathrm{cov}}^{\mathrm{JT}}$) via the standard two-factor tensor construction [28, 29] has

$$\|H_{\mathrm{JT}}\|_{\mathrm{ren}} \;\le\; \frac{1}{\gamma_{\mathrm{JT}}} \;+\; C_{\mathrm{cov}}^{\mathrm{JT}} \Big(1 + \frac{\big\|K^{\mathrm{JT}}\big\|}{\gamma_{\mathrm{JT}}}\Big). \tag{79}$$

This bound is uniform in λ by assumption (A4′) and the uniform-gap condition (A2), satisfying condition (A5) of Theorem 2.

Remark 7 (On explicit total-complex homotopy formulas). For a two-row bicomplex $\mathcal{B}^{p,q}$ with $q \in \{0,1\}$, the explicit form of a total contracting homotopy requires careful bigraded sign tracking; standard references ([28] Ch. VIII; [29]) give the general construction. The Künneth acyclicity argument suffices for the structural claim $H^n_Q = 0$; the quantitative bound (79) suffices for Theorem 2(e). In this paper we do not state an explicit closed-form identity $QH_{\mathrm{JT}} + H_{\mathrm{JT}}Q = \mathbf{1}$ to avoid sign ambiguities; the existence and norm bound are all that the theorem requires.

Boundedness of the homotopy. By (21) of Remark 4 applied with $\gamma = \gamma_{\mathrm{JT}}$ (the Schwarzian spectral gap) and $C_{\mathrm{cov}} = C^{\mathrm{JT}}_{\mathrm{cov}} \le 2$:

$$\|H_{\mathrm{JT}}\| \;\le\; \frac{1}{\gamma_{\mathrm{JT}}} \;+\; C^{\mathrm{JT}}_{\mathrm{cov}} \Big(1 + \frac{\big\|K^{\mathrm{JT}}\big\|}{\gamma_{\mathrm{JT}}}\Big). \tag{80}$$

Both $C^{\mathrm{JT}}_{\mathrm{cov}}$ and the maximum birth–death rate $\big\|K^{\mathrm{JT}}\big\|$ are bounded combinatorial constants independent of the cutoff λ (the rate magnitudes are bounded by the chosen bath spectral density times a finite matrix-element factor; the gap γ_{JT} is uniformly bounded below by assumption (A2)). Consequently $\sup_\lambda \|H_{\mathrm{JT}}\| < \infty$, satisfying condition (e) of Theorem 2.

Conclusion: conditional acyclicity. Under the cover-multiplicity assumption (A4′) and the uniform-gap assumption (A2), the Künneth argument (78) gives $H^n_Q = 0$ for all $n \ge 0$ on V_0^{JT}-valued cochains. In particular $H^2_Q = 0$, instantiating (A5)/(e) of Theorem 2. Combined with the centering domain restriction (A3′) and Proposition 2 from §5.5, and the resolvent bound from §5.4, the JT model *instantiates* all five assumptions of Theorem 2 at finite regulator λ, with (A3′) serving as the domain assumption that makes the centering condition a theorem rather than an axiom. The continuum limit $\lambda \to 0$ and the uniform-gap renormalization remain open; see §8 Open Problems (i)–(ii).

6 Comparison of the four closures

Table 1 compresses the four worked closures into one comparison view: JT gravity in the main body (§5) and three further regulators in the appendices (AdS–Rindler in App. A, AdS/CFT code in App. B, spin-network in App. C). Two observations are worth flagging.

Structural unity is a feature, not a defect. All four regulators are instances of the same closure schema (§2.4) with the same five assumptions. What differs across the rows of Table 1 is exclusively the physical origin of each ingredient — record set, microscopic centering identity, cover/refinement structure — not the abstract mathematical machinery. Theorem 2 was proved once, regulator-independently; the four regulators are not four independent proofs of the same claim, but four physically distinct realizations of the same abstract template. The portability of the abstract template across JT gravity, AdS/CFT, operator-algebra QEC, and loop-gravity corners is itself a structural claim of the paper: any candidate quantum-gravity theory in which a finite record sector and a primitive erasure generator can be identified, together with a microscopic identity that forces centering, falls within the CPE template.

Model	Records R_λ	Erasure K_λ	Anomaly-cancellation identity	Causal complex	Gap γ_λ	CPE closure failure mode
JT (§5)	Schwarzian energy + horizon-dilaton bins	Davies-type birth–death on energy bins	SL(2,$\mathbb{R}$) Ward identity on non-identity sector $\mathcal{D}_{\mathrm{JT}}$ + (A3′) [9]	Koszul 2-term ⊗ Čech cover of 1D boundary	$\frac{1}{2}\Phi_K^2$ (Cheeger)	Anomalous SL(2,$\mathbb{R}$) identity primary (failure of A3′)
AdS–Rindler (App. A)	Area + modular-energy + wedge-mode bins	Davies generator on modular time (KMS)	First law + JLMS on domain $\mathcal{D}_{\mathrm{Rindler}}$ [12, 13]	Koszul 2-term ⊗ causally convex cover	$4\pi T h_{\min}$ (QNM) [31]	Response outside $\mathcal{D}_{\mathrm{Rindler}}$ or bulk operator unreconstructable
AdS/CFT code (App. B)	Center labels α of operator-algebra code	Syndrome-mixing recovery channel	Gauge–logical dichotomy (Prop. 4)	Koszul 2-term ⊗ reconstruction cover	Cheeger gap of syndrome graph	Logical operator outside subregion algebras
Spin corner (App. C)	Punctures + intertwiners + shape bins	Local-move Markov chain	Peter–Weyl on non-singlet sector + (A3-sing) [21]	Koszul 2-term ⊗ refinement-category nerve	$\frac{1}{2}\Phi_K^2$ (Cheeger)	Persistent singlet anomaly (failure of A3-sing)

Table 1: Side-by-side comparison of the four model closures. All four follow the same structural template (finite record system + Markovian erasure + microscopic centering identity + explicit homotopy on the causal complex), but differ in the physical origin of each ingredient and in the precise failure mode that a violation of $H_Q^2 = 0$ encodes. The contracting homotopy h_λ has the uniform form (79), (116), (136), (160) in the four cases respectively.

Model-specific failure modes. The last column of Table 1 lists, for each regulator, the precise obstruction to CPE closure. In the two-row Koszul bicomplex, $H^n_Q = 0$ for all $n \geq 0$ follows by Künneth whenever both the vertical Koszul complex and the horizontal Čech/nerve complex are acyclic; the listed failure modes are therefore not failures of $H^2_Q = 0$ per se, but failures of the conditions that guarantee acyclicity — most commonly a failure of the stationary anomaly condition (identity-primary contamination in JT, logical-sector anomaly in code, singlet anomaly in spin-network) or a failure of primitivity/gap uniformity. CPE turns these physical obstructions into concrete, model-specific diagnostics rather than opaque spacetime anomalies.

7 Simulation protocol: a SYK/JT analog target

The worked examples change the natural target for testing CPE. A desktop qubit test is unlikely to see gravitational edge records directly. Better simulation targets are: (i) analog horizon systems where quasi-normal-mode damping and edge records can be engineered; (ii) SYK/JT-type quantum simulators where Schwarzian relaxation and finite code subspaces can be probed; (iii) tensor-network or holographic-code simulations where center labels and recovery maps are explicit; and (iv) spin-network or lattice-gauge models where puncture/edge labels and refinement maps can be enumerated. In each case the CPE signature is not a generic nonlinear drift, but a transient that is centered in the stationary record measure, decays at the Markov-chain gap rate γ_K, and disappears after record equilibration. A persistent stationary drift is not a CPE signal; it is a Ward anomaly and a failure of the mechanism (Theorem 1).

This section develops target (ii) — the SYK/JT analog simulator — in enough quantitative detail to define a concrete observable, a preparation protocol, a discrimination criterion, and a finite-sampling noise model. We frame the section as a *simulation protocol* for analog quantum simulators rather than an experimental prediction for any particular near-term hardware: the protocol specifies what observable to measure, how to prepare the initial state, what signature distinguishes CPE from generic dephasing, and what shot budget is needed. Whether any specific platform (transmon array, photonic lattice, trapped-ion register) achieves the required post-selective resolution at the relevant temperature is a separate hardware question, addressed only insofar as the protocol's resource demands are stated explicitly. Targets (iii) and (iv) admit analogous treatments using the code and spin-network constructions of §§B–C.

7.1 The SYK/JT analog-simulator target

The Sachdev–Ye–Kitaev (SYK) model [32–34] consists of N Majorana fermions ψ_i ($i = 1, \ldots, N$) with all-to-all quartic interactions J_{ijkl} drawn i.i.d. from a Gaussian distribution with mean zero and variance $3!\, J^2/N^3$:

$$H_{\mathrm{SYK}} = \frac{1}{4!} \sum_{i<j<k<l} J_{ijkl}\, \psi_i \psi_j \psi_k \psi_l. \tag{81}$$

At large N with $\beta J \gg 1$, the low-energy dynamics is described by the JT/Schwarzian effective action of §5, and the boundary energy E plays the role of the record label. We partition the allowed energy interval into $L+1$ bins:

$$R^{\mathrm{SYK}}_\lambda = \{0, 1, \ldots, L\}, \qquad \text{bin } r\text{: } E \in [r\Delta E,\, (r{+}1)\Delta E), \tag{82}$$

with bin width $\Delta E \sim J/\sqrt{N}$ (one thermal energy fluctuation unit). The stationary distribution $\mu^{\mathrm{SYK}}_r \propto \int_{E_r}^{E_{r+1}} \rho_{\mathrm{SYK}}(E) e^{-\beta E}\, \mathrm{d}E$ weights each bin by the Bethe/Schwarzian density of states

$\rho_{\mathrm{SYK}}(E) \propto e^{2\pi\sqrt{2E/J}}$ [34]. The Markov generator K^{SYK} is the Davies-type thermalization chain from (55)–(56) with rates computed from (54); its spectral gap satisfies $\gamma_K \geq \frac{1}{2}\Phi_K^2 > 0$ by the argument of §5.4.

7.2 The CPE observable: record-conditional two-point cumulant

For a state ρ of the N Majoranas, define the two-point function

$$G[\rho](\tau) := -\frac{1}{N}\sum_{i=1}^{N}\langle \mathcal{T}\,\psi_i(\tau)\psi_i(0)\rangle_\rho, \qquad \tau \in [0,\beta], \tag{83}$$

where $\langle\cdot\rangle_\rho = \mathrm{tr}(\rho\,\cdot)$ and $\mathcal{T}$ is imaginary-time ordering. The *record-conditional* two-point function is

$$G_r(\tau) := G\left[\frac{\Pi_r \rho \Pi_r}{\mathrm{tr}(\Pi_r \rho)}\right](\tau), \tag{84}$$

where Π_r is the spectral projector onto energy bin r. A CPE-compatible nonlinear response in this system has the form $\mathcal{N}_r[\rho] = \tilde{\alpha}_r \cdot (G_r(\tau_0) - G_\infty(\tau_0)) \cdot A$ for some fixed observable A, centred scalar couplings $\tilde{\alpha}_r$ (with $\sum_r \mu_r \tilde{\alpha}_r = 0$ by (A3)), and $G_\infty(\tau_0) := \sum_r \mu_r G_r(\tau_0)$.

The *residual cumulant* at time t is

$$e_t(\tau_0) := \Big|\sum_r \omega_t(r)\,\tilde{\alpha}_r\,(G_r(\tau_0) - G_\infty(\tau_0))\Big|, \tag{85}$$

where $\omega_t(r) = (e^{tK^{\mathrm{SYK}}}\nu_0)_r$ starts from a non-stationary $\nu_0 \neq \mu^{\mathrm{SYK}}$. If quantum mechanics is exactly linear, then $G_r = G_\infty$ for all r and $e_t \equiv 0$; a nonzero e_0 encodes the initial state-dependence that CPE predicts will relax at rate γ_K. The three-state numerical illustration of §3.5 is the simplest instance of this observable, with $\tilde{\alpha} = (-1, 0, +1)$ chosen on the slow eigenmode of K so that e_t decays at exactly the chain gap $\gamma = 1$.

7.3 Preparation protocol: energy-bin post-selection

A non-stationary initial distribution $\nu_0 \neq \mu^{\mathrm{SYK}}$ can be prepared by two complementary methods.

Off-equilibrium quench. Prepare the SYK system in its ground state $|\Omega\rangle$ or at inverse temperature $\beta' \gg \beta$. The initial energy distribution $\nu_0(r) = \langle\Omega|\Pi_r|\Omega\rangle$ is concentrated at low-energy bins, far from the thermal μ. The system is then coupled to the thermalization bath (implementing K^{SYK}) and the record distribution evolves as $\omega_t = e^{tK^{\mathrm{SYK}}}\nu_0$.

Post-selective energy readout. Prepare an arbitrary state and measure the energy at resolution ΔE, post-selecting on outcome r_0; this yields $\nu_0 = \delta_{r,r_0}$. The subsequent evolution ω_t starts from a single bin, providing the cleanest test of the spectral gap. For $N \sim 8$–16 Majorana modes, the required resolution is $\Delta E \sim J/\sqrt{N} \approx J/3$ (for $N = 10$). Existing SYK analog proposals [33, 34] target this readout regime as a long-term goal; whether any specific near-term realization achieves the necessary post-selective energy resolution at the temperatures of interest is a hardware-dependent question we do not settle here. The protocol below is stated as a target for analog simulators that reach the regime, not as an immediate near-term experiment.

7.4 Discrimination criterion: gap scaling versus ordinary decoherence

The central CPE prediction is exponential decay at the chain gap:

$$e_t(\tau_0) \;\approx\; e_0(\tau_0)\, e^{-\gamma_K t}, \tag{86}$$

with γ_K determined by the SYK thermalization chain, not by any external dephasing bath. Two signatures discriminate this from ordinary decoherence.

Temperature scaling. The CPE gap γ_K is controlled by the lowest Schwarzian quasi-normal mode $\lambda_{\mathrm{QNM}} \sim 2\pi T \cdot f(\beta J)$, a universal function of βJ [8, 31]. Standard environmental dephasing produces a decay rate $\Gamma_{\mathrm{deph}} \propto T^{\nu}$ with an exponent ν set by the bath spectral density. Plotting the measured decay rate of e_t against temperature T (at fixed J) distinguishes the two: CPE follows the Schwarzian quasi-normal-mode curve, while dephasing follows a different power law.

Initial-state independence. The CPE decay rate γ_K is the second eigenvalue of K^{SYK}, independent of ν_0. Many environmental-decoherence channels produce effective rates that depend on the initial state when the Lindblad operators are not of Davies/KMS form. Verifying that the decay rate is the same for both preparation protocols of §7.3 provides an independent check that the relaxation is governed by the Markov chain.

7.5 Magnitude estimate and finite-sampling noise model

Signal amplitude. The bin-to-bin fluctuation of the conditional two-point function is, to leading order in $1/N$,

$$\delta G := \max_r |G_r(\tau_0) - G_\infty(\tau_0)| \;\approx\; \frac{1}{\sqrt{N}}\, |G_\infty(\tau_0)|. \tag{87}$$

This estimate follows from the central-limit-theorem scaling of the energy fluctuation within one thermal unit: $\Delta E_{\mathrm{rms}} \sim J/\sqrt{N}$ implies $G_r - G_\infty \approx (\partial G/\partial\beta)\cdot(\partial\beta/\partial E)\cdot\Delta E_{\mathrm{rms}}$, which is $O(G_\infty/\sqrt{N})$. At $\tau_0 = \beta/2$, $N = 10$, $\beta J = 5$: $|G_\infty(\beta/2)| \approx (\pi/(\beta J))^{1/2} \approx 0.79$ in the conformal normalisation [34], giving $\delta G \approx 0.25$. The initial residual cumulant amplitude is $e_0 \approx |\tilde{\alpha}| \cdot \delta G \approx 0.25|\tilde{\alpha}|$.

Shot-noise threshold. Each single-shot measurement of $G_r(\tau_0)$ from N Majorana pairs has statistical error $O(1/\sqrt{N})$; for M_r shots conditioned on record bin r, the estimator standard deviation is

$$\sigma_G^{(r)} = \frac{1}{\sqrt{M_r N}}. \tag{88}$$

The signal-to-noise condition $e_0 > 3\sigma_G$ at $t = 0$ requires

$$M_r > \frac{9}{N\,(\delta G)^2\,\tilde{\alpha}_r^2}. \tag{89}$$

For $N = 10$, $\delta G = 0.25$, $|\tilde{\alpha}_r| = 1$: $M_r^{\min} \approx 14$ shots per bin. To see the decay to $t = 1/\gamma_K$ (where $e_t \approx 0.37\, e_0$): $M_r^{\min} \approx 100$ shots per bin. With $L + 1 \sim 6$ energy bins, the total shot budget is $M_{\mathrm{total}} \lesssim 600$ shots — within reach of near-term quantum simulators with $N \lesssim 16$ Majorana modes and $M \sim 10^3$ shots per run.

Systematic errors. Two systematic effects must be controlled. (*a*) *Bin-width bias*: coarser ΔE reduces δG but degrades centering precision; the choice $\Delta E \sim J/\sqrt{N}$ from (82) is optimal. (*b*) *Non-Markovian corrections*: the Davies/van Hove approximation of §5.4 is valid at weak coupling $\varepsilon^2 t \lesssim 1$; for longer observation times, higher-order memory corrections could modify the decay envelope. Both can be estimated and bounded using standard quantum process tomography for $N \lesssim 20$ Majorana systems.

7.6 Distinguishing CPE from generic dephasing in a realistic simulator

In any realistic analog simulator, several relaxation channels coexist alongside the CPE-relevant Markov erasure: the simulator's own thermalization to its bath, ordinary dephasing from environmental noise, finite-size revivals from the bounded SYK spectrum, and residual coherent errors from imperfect Hamiltonian implementation. None of these is the CPE signature, but each can mimic an exponential decay of $e_t(\tau_0)$ over a limited time window. The protocol below isolates CPE by combining two independent discrimination strategies:

(i) *Record-conditioned preparation.* Generic dephasing produces a decay of e_t that does *not* depend on the initial record bin r_0 chosen in §7.3: any starting state relaxes to the thermal state at roughly the same rate. CPE produces a decay whose rate is the chain gap γ_K *independent of* r_0, but whose initial amplitude $e_0(\tau_0)$ depends sharply on r_0 (concentrated single-bin preparation gives the cleanest signal). Varying r_0 over several bins and checking that the fitted decay rate is constant while the amplitude varies as predicted by the eigenmode decomposition is the strongest single test.

(ii) *Temperature-scaling.* As in §7.4, the CPE gap γ_K tracks the Schwarzian QNM curve $\lambda_{\mathrm{QNM}} \sim 2\pi T \cdot f(\beta J)$ in temperature, while ordinary dephasing follows a bath-spectral power law $\Gamma_{\mathrm{deph}} \propto T^{\nu}$. A two-parameter fit of $\log \gamma_K(T)$ against $\log T$ in the regime $\beta J \gg 1$ separates the two functional forms.

Neither discrimination criterion is decisive in isolation: a hardware-specific bath structure could conspire to produce a power law numerically close to $f(\beta J)$ in a limited temperature window, and a preparation protocol with hidden dependence on r_0 could mimic the eigenmode amplitude structure. Together, however, the two criteria are restrictive: any putative CPE detection must satisfy both, and a detection that satisfies neither is not a CPE signal — it is exactly the kind of generic relaxation that the worked-model construction was designed to be distinguishable from.

8 Conclusion

The Causal Preparation Erasure mechanism has two logically separate parts, and they play very different roles. The first part is mathematical: zero-mean nonlinear responses in an erasing record sector are K-coboundaries (Lemma 1) and vanish from record-erased operational dynamics up to controlled boundary and transport errors (Theorem 2, equation (30)). This part is closed: it rests on finite Poisson equations, conductance-based resolvent estimates (Lemma 2), and a homological-perturbation-theory bound on the Maurer–Cartan series (Proposition 1), all of which are uniform in the cutoff λ once the standard projective tightness assumptions are imposed.

The second part is physical: a quantum-gravity model must supply, as input, the microscopic identity that forces the centering condition $\sum_r \mu_r \mathcal{N}_r = 0$. Without such an input, the no-go theorem (Theorem 1) shows that records and erasure cannot do the work alone. The four worked regulators

(JT in §5; AdS–Rindler, code, and spin-network in Appendices A–C) are existence proofs that the required identity can be implemented in physically distinct ways:

- JT gravity closes the mechanism through the SL(2,$\mathbb{R}$) Ward identity of the Schwarzian action.
- AdS–Rindler wedges close it through the first law of entanglement combined with the JLMS identity.
- Finite-cutoff holographic codes close it through the gauge–logical dichotomy of operator-algebra QEC.
- Spin-network corners close it through the Gauss/closure constraint via Peter–Weyl group averaging *on the non-singlet sector*; the residual singlet anomaly is excluded by the additional assumption (A3-sing) of §C.5.

In each model, all five assumptions (A1)–(A5) of Theorem 2 are explicitly *instantiated* at finite regulator and shown to be mutually consistent, including an explicit contracting homotopy on the relevant causal bicomplex. Which conditions follow from microscopic symmetries and which are model-specific domain restrictions or modelling inputs is stated explicitly in each case.

What this paper does *not* claim. We do not claim that the real universe satisfies the closure conditions. We do not claim that the four regulators are physically realistic models of quantum gravity — they are deliberately simplified existence proofs in which every ingredient is finite and computable. The strong claim is conditional:

> *In any finite quantum-gravity regulator in which assumptions (A1)–(A5) of Theorem 2 are satisfied, record-erased low-energy dynamics is affine-linear up to the explicit error bound (30). Whether a given candidate regulator satisfies these assumptions — in particular whether its Markov erasure generator has a λ-uniform gap (A2) and its stationary anomaly genuinely vanishes from a microscopic identity (A3) — is a model-specific question not settled by this theorem.* (90)

This is the precise sense in which CPE proposes a conditional derivation of quantum linearity: affine-linearity is a theorem in any finite regulator that satisfies (A1)–(A5), and the no-go theorem identifies exactly what must be verified in each candidate regulator for CPE to apply. Quantum linearity is not derived from nothing; it is reduced to a finite list of microscopic identities that a theory of quantum gravity may or may not satisfy.

Limitations. Beyond the points listed above, three structural limitations should be noted explicitly.

- *Markov rates are inputs, not derivations.* In each model the Markov generator K_λ is supplied as part of the data tuple, with explicit rates that depend on the choice of bath/coupling/regulator. The Davies/van Hove construction [30] guarantees that *some* Markovian reduction exists, but the specific rates are not determined by the underlying gravity theory alone (see Remark 6). Establishing the specific rates from a first-principles model is an open problem in each case.
- *The four models share one mathematical mechanism.* As discussed in §6, the closure mechanism reduces to a single abstract structure (finite primitive Markov chain + Drazin inverse + double-complex homotopy via homological perturbation). The four models differ in physical interpretation but not in mathematical content. This is a positive structural feature for showing portability, but it means the four models are not four independent existence proofs of the abstract claim.

- *The empirical signature requires access to the record measure.* The CPE prediction — a transient response decaying at rate γ_λ — requires that the stationary record distribution μ_λ be operationally accessible. In laboratory analog experiments this is plausible (analog horizons with engineered records); in actual gravitational systems (e.g., astrophysical black holes) it is not currently realistic.

Open problems. Five model-dependent questions remain open and deserve separate treatment:

(i) *Uniform renormalization.* Each model section assumes uniformity of the resolvent bound, the homotopy norm, and the projective coarse-graining error across the family of cutoffs. Establishing this rigorously in each model is a renormalization problem in its own right, controlled by Lemma 2 only when the family of erasure chains has λ-independent conductance.

(ii) *Continuum limit.* Even when uniformity holds at each finite λ, taking $\lambda \to 0$ involves a delicate limit of the Künneth-acyclicity construction and may require additional structure beyond finite-dimensional vector spaces (e.g., the type-III modular structure of the continuum local algebra [35, 36]).

(iii) *Domain of the state-to-bulk map in AdS–Rindler.* The first-law derivation of centering for the AdS–Rindler regulator (App. A) requires the state-dependent JLMS identity to hold on the admissibility domain $\mathcal{D}_{\mathrm{Rindler}}$ (Definition 5). Whether physically realised nonlinear responses in candidate AdS/CFT regulators land inside $\mathcal{D}_{\mathrm{Rindler}}$ at the required order in G_N, and how the domain extends beyond the perturbative neighborhood of the modular Gibbs state, is a model-specific question we do not settle here; a quantum-extremal-surface refinement [37] of the present argument is one natural next step.

(iv) *Non-equilibrium erasure.* The closure theorem as stated assumes the erasure generator is time-independent or only adiabatically varying. Extending the bound to genuinely non-equilibrium erasure (e.g., a moving entanglement wedge, a dynamically refining spin network) requires a generalization of the moving-potential identity (40) that is currently only sketched in the transport-defect subsections of each model.

(v) *Characterization of the model-specific centering domains.* The JT centering proposition (Proposition 2) is restricted to the non-identity Schwarzian primary domain $\mathcal{D}_{\mathrm{JT}}$ (Definition 4) by assumption (A3′), and the spin-network derivation requires the singlet-exclusion assumption (A3-sing) of §C.5. Whether every physically realized horizon response of the JT regulator lies in $\mathcal{D}_{\mathrm{JT}}$ — and whether back-reaction at order G_N or matter couplings beyond leading order preserve (A3′) by excluding state-dependent identity-sector counterterms — is a JT-specific question. The analogous spin-network question is whether the four corner-scalar failure modes (corner charge, boundary Hamiltonian, chemical potential, superselection parameter) can be ruled out in a specific spin-network regulator. The spin-network model remains the most model-dependent of the four regulators in the present construction.

None of these open problems threatens the structural validity of the CPE mechanism, but each is essential to converting the four worked regulators into a complete physical theory.

The decisive empirical signature. The CPE prediction is sharp: in any regulator in which all five conditions hold, the operational nonlinear response is a *transient* that is centered in the stationary record measure, decays with the erasure gap γ_λ, and disappears after record equilibration on timescales $1/\gamma_\lambda$. A persistent stationary drift is not a CPE signal; it is, by Theorem 1, the

signature of a Ward anomaly and a failure of the mechanism in the relevant regulator. This converts the empirical search for low-energy nonlinearity into a search for transient centered responses with a specific gap-controlled decay envelope, rather than for generic deviations from linear quantum mechanics.

A AdS-Rindler entanglement wedge

A.1 Microscopic setup

Let A be a ball-shaped region in the vacuum of a holographic CFT. The vacuum modular Hamiltonian is local:

$$K_A^{\mathrm{CFT}} = 2\pi \int_A \mathrm{d}^{d-1}x \, \frac{R^2 - |x - x_0|^2}{2R} \, T_{00}(x). \tag{91}$$

The dual bulk region is an AdS-Rindler entanglement wedge. The Ryu-Takayanagi and covariant HRT prescriptions identify the leading entropy with an extremal area [11, 38]. JLMS gives the operator relation, within a code subspace,

$$K_A^{\mathrm{CFT}} = \frac{\widehat{A}_\chi}{4G_N} + K_{\mathrm{bulk}}^{\mathrm{wedge}} + O(G_N^0 \text{ counterterms}), \tag{92}$$

where χ is the extremal surface [12]. This is precisely a modular information-geometric setting for CPE.

A.2 Record algebra

Choose a finite regulator λ consisting of area bins a, modular-energy bins q, and a finite set of low-lying wedge relaxation modes $m_1, \ldots, m_L$. Define

$$R_\lambda^{\mathrm{Rindler}} = \{r = (a, q, m_1, \ldots, m_L)\}. \tag{93}$$

The record algebra is

$$\mathfrak{Z}_\lambda^{\mathrm{Rindler}} = \ell^\infty(R_\lambda^{\mathrm{Rindler}}). \tag{94}$$

The generalized entropy assigned to a record is

$$S_{\mathrm{gen}}(r) = \frac{A_a}{4G_N} + S_{\mathrm{bulk},q,m} + S_{\mathrm{edge},r} + S_{\mathrm{ct}}. \tag{95}$$

A local preparation in A changes $\delta\langle K_A^{\mathrm{CFT}}\rangle$. By (92), unless there is exact compensation between area and bulk modular energy, it changes the record label (a, q, m).

A.3 Erasure generator from modular relaxation

Use modular time s generated by K_A^{CFT}. A finite Davies-type generator for the record labels is

$$K_{rs} = \sum_\alpha |\langle s|V_\alpha(\omega_{sr})|r\rangle|^2 \, \widehat{C}_\alpha(\omega_{sr}), \qquad r \neq s, \tag{96}$$

where $\omega_{sr} = k_s - k_r$ is the modular-energy difference. The KMS condition in modular time gives

$$\widehat{C}_\alpha(-\omega) = e^{-2\pi\omega} \widehat{C}_\alpha(\omega). \tag{97}$$

Thus a stationary distribution is

$$\mu_r = \frac{1}{Z_\lambda} \exp\left(S_{\text{edge}}(r) - 2\pi k_r\right), \tag{98}$$

or, equivalently, the finite-bin projection of the modular Gibbs state. If the graph of nonzero rates in (96) is connected, K is primitive. Since R_λ is finite, the zero-mean resolvent is bounded by $1/\gamma_{\text{Rindler}}$, with γ_{Rindler} the first nonzero eigenvalue in the reversible case or the exponential contraction rate in the non-normal case.

In BTZ or thermal AdS_3 reductions one may further identify some of the rates with quasinormal-mode damping. For BTZ modes,

$$\omega_{L,k,n} = k - 4\pi i T_L(n + h_L), \qquad \omega_{R,k,n} = -k - 4\pi i T_R(n + h_R), \tag{99}$$

so $\gamma_{\sigma,n} = 4\pi T_\sigma(n + h_\sigma)$ controls relaxation; the match between BTZ quasinormal frequencies and poles of retarded CFT correlators is standard [31].

A.4 Stationary anomaly from relative entropy and JLMS

We now derive the centering condition $\Pi_\mu \mathcal{N} = 0$ for the Rindler model from two microscopic inputs: the first law of entanglement, and the JLMS bulk/boundary modular identity (92).

Step 1: relative entropy and modular Hamiltonian. For nearby states ω and σ on the boundary algebra of A, the Araki relative entropy satisfies the first law

$$S_{\text{rel}}(\omega\|\sigma)\big|_{\omega\to\sigma} \;=\; \Delta\langle K_A^{\text{CFT}}\rangle - \Delta S_A \;=\; 0 \quad \text{at first order in } \omega - \sigma, \tag{100}$$

where $S_A = -\operatorname{tr}(\rho_A \log \rho_A)$ is the von Neumann entropy on A and K_A^{CFT} is the boundary modular Hamiltonian (91) (not to be confused with the Markov generators K_λ that play a different role throughout the paper). Equivalently, $\delta S_A = \delta\langle K_A\rangle$ for arbitrary first-order perturbations [13, 14]. By construction the modular Gibbs state $\sigma_\mu \propto e^{-K_A}$ is the unique state at which this identity becomes a stationary equilibrium statement. Its discretization at cutoff λ gives the stationary distribution (98), $\mu_r \propto e^{S_{\text{edge}}(r) - 2\pi k_r}$.

Step 2: JLMS lifts the first law to the bulk record. The JLMS operator identity (92) lifts K_A^{CFT} to a sum of an area term and a bulk modular Hamiltonian inside the code subspace:

$$K_A^{\text{CFT}} \;=\; \frac{\widehat{A}_\chi}{4G_N} \;+\; K_{\text{bulk}}^{\text{wedge}} \;+\; O(G_N^0). \tag{101}$$

Combined with the first law (100), this implies that the variation of the generalized entropy along an allowed first-order perturbation is

$$\delta S_{\text{gen}}(r) \;=\; \delta\Big(\tfrac{A_r}{4G_N} + S_{\text{bulk},q,m} + S_{\text{edge},r}\Big) \;=\; \delta\langle K_A^{\text{CFT}}\rangle \;=\; \delta(2\pi k_r) + O(\delta^2), \tag{102}$$

where k_r is the modular-energy bin label assigned to the record r. The right-hand side is exactly the part of the stationary distribution $\mu_r \propto e^{S_{\text{edge}}(r) - 2\pi k_r}$ that depends on r.

Step 3: from the first law to centering. We must be careful to distinguish two questions: (a) which responses are *defined* to be first-law admissible, and (b) which class of physically realized responses *are* first-law admissible at leading order in G_N. The non-trivial physical input from JLMS is the answer to (b), not (a).

(a) Define a response $\mathcal{N}_r[\omega]$ to be *first-law admissible* at cutoff λ if the corresponding state perturbation $\delta\omega$ generated by $\mathcal{N}$ preserves the first law (102) at first order, i.e., $\delta S_{\rm gen}(r) = \delta\langle K_A^{\rm CFT}\rangle_r$ holds record-by-record. This is a definition, not a derivation.

(b) The physical input is the JLMS theorem [12]: for *any* bulk perturbation in the code subspace at leading order in G_N, the resulting boundary perturbation is first-law admissible in the sense of (a). Equivalently, the only first-law-violating responses live outside the code subspace and represent non-perturbative effects. This is non-trivial physical content: it says that within the perturbative bulk reconstruction regime, every allowed response is admissible.

Combining (a) and (b): for a response $\mathcal{N}$ that arises from a bulk perturbation in the code subspace at order G_N^0,

$$\sum_r \mu_r\, \mathcal{N}_r[\omega] \;=\; \sum_r \mu_r\, \left(\delta S_{\rm gen}(r) - \delta\langle K_A^{\rm CFT}\rangle_r\right)\cdot \mathcal{M}[\omega] \;=\; 0, \tag{103}$$

where $\mathcal{M}[\omega]$ is the state-dependent kernel and the term in parentheses vanishes *record-by-record* by JLMS (via (b)) combined with the first law (via (a)). This is the JLMS-based derivation of the centering condition: the centering is the consequence, the input is JLMS + first law.

The most general first-law-admissible response decomposes against the centered bin labels:

$$\mathcal{N}_r[\omega] = \alpha(k_r - \bar{k}_\mu)\mathcal{V}[\omega] + \beta(A_r - \bar{A}_\mu)\mathcal{W}[\omega] + \sum_\ell \gamma_\ell(m_{\ell,r} - \bar{m}_{\ell,\mu})\mathcal{U}_\ell[\omega] + \mathcal{N}_r^{\perp}[\omega], \tag{104}$$

where each label is centered by construction, $\sum_r \mu_r(A_r - \bar{A}_\mu) = 0$ etc., and $\mathcal{N}^\perp$ collects the remaining (Schwarzian-type primary) content with $\sum_r \mu_r \mathcal{N}_r^\perp = 0$ by an analogue of (63) for the modular Gibbs state. Therefore

$$\Pi_\mu \mathcal{N} \;=\; \sum_r \mu_r\, \mathcal{N}_r \;=\; 0. \tag{105}$$

Failure mode. The derivation breaks down if $\mathcal{N}$ contains a piece $a\mathcal{V}[\omega]\cdot \mathbf{1}_{\mathfrak{Z}_\lambda^{\rm Rindler}}$ that is constant in r — equivalently, a state-dependent shift of the generalized entropy that is record-independent. Such a term would violate the first law of entanglement at first order in ε, hence cannot arise from any allowed bulk perturbation consistent with JLMS. This is the precise sense in which JLMS forces $\Pi_\mu\mathcal{N} = 0$ in this regulator.

A.5 Domain and order of the first-law-admissibility input

The argument of §A.4 relies on first-law admissibility of the nonlinear response, which in turn rests on the JLMS identity holding for state-dependent perturbations. Standard JLMS [12] is stated for fixed first-order operator-level perturbations of a fixed background state; the present construction needs slightly more, because $\mathcal{N}[\omega]$ is itself state-dependent. We make the resulting domain and order of validity explicit.

The state-to-bulk map. Given a record-conditional response $\mathcal{N}_r[\omega]$ with ω in the code subspace $\mathcal{H}_{\text{code}} \subset \mathcal{H}_{\text{CFT}}$, define a candidate bulk perturbation via the dictionary

$$\delta\phi_r[\omega] \;:=\; \Phi_{\text{dict}}(\mathcal{N}_r[\omega]), \tag{106}$$

where $\Phi_{\text{dict}} : \mathcal{M}_{\text{CFT}} \to \mathcal{M}_{\text{bulk}}^{\text{code}}$ is the entanglement-wedge reconstruction map at leading order in G_N [16]. We say $\mathcal{N}$ is *first-law admissible* on a domain $\mathcal{D} \subseteq \mathcal{H}_{\text{code}}$ if, for every $\omega \in \mathcal{D}$, the candidate $\delta\phi_r[\omega]$ lies in the code-subspace algebra $\mathcal{M}_{\text{bulk}}^{\text{code}}$ and the JLMS operator identity (92) holds when both sides are expanded to first order in $\delta\phi$ around the state ω.

Order of validity. Two small parameters control the construction. (i) The bulk Newton constant: standard JLMS holds at leading order $O(G_N^{-1})$ for the area term and $O(G_N^0)$ for the bulk modular term, with corrections $O(G_N^0$ counterterms) and $O(G_N)$ subleading [12, 14]. (ii) The nonlinearity coupling ε of the CPE response: $\mathcal{N}$ enters at order ε and we work to $O(\varepsilon)$. The state-dependent JLMS we require holds at the same orders — $O(G_N^{-1})$ for the area term, $O(G_N^0)$ for the bulk modular term, $O(\varepsilon)$ in the nonlinearity — and is established at this combined order in the same code-subspace setting used for state-independent JLMS, since the proof of JLMS via the bulk replica trick [14] treats the bulk modular Hamiltonian as an operator equation and does not require $\delta\phi$ to be state-independent.

Domain $\mathcal{D}$. The admissible domain $\mathcal{D}$ for which (106) is meaningful and JLMS holds is:

(i) ω in the code subspace $\mathcal{H}_{\text{code}}$: outside it, the dictionary Φ_{dict} does not act and JLMS does not apply;

(ii) ω within the perturbative bulk reconstruction regime: $\|\omega - \sigma_\mu\| \le c\sqrt{G_N}$ for some c, where σ_μ is the modular Gibbs state of the chosen ball. Beyond this distance, higher-order JLMS corrections that we have not bounded can dominate;

(iii) $\mathcal{N}_r[\omega]$ Fréchet-differentiable in ω at σ_μ, so that the linearization in $\delta\omega$ defining $\delta\phi_r[\omega]$ is well-defined.

A response $\mathcal{N}$ on $\mathcal{D}$ in this sense is what (a)+(b) of §A.4 require.

Domain and order of validity. The argument uses only the leading-order (G_N^{-1}, G_N^0) JLMS identity on the perturbative domain $\mathcal{D}$. Responses that take states outside $\mathcal{H}_{\text{code}}$, that produce $\delta\phi$ with $O(G_N)$ back-reaction on the extremal surface, or that lie in the non-perturbative regime are outside this scope; a quantum-extremal-surface refinement [37] would be needed in those cases. The domain $\mathcal{D}$ is a perturbative neighborhood of σ_μ, not the full code subspace. Whether physically realized responses land inside $\mathcal{D}$ is the model-specific question of Open Problem (iii).

Rindler centering as a domain-restricted Proposition. Combining §A.4 Step 3 with the domain $\mathcal{D}$ above, we state the centering claim with its restriction visible in the proposition body rather than only in the surrounding prose.

Definition 5 (The Rindler admissible domain $\mathcal{D}_{\text{Rindler}}$)**.** Let $\mathcal{D}_{\text{Rindler}} \subset$ {record-conditional responses $\mathcal{N}_r[\omega]$} denote the subclass for which:

(i) $\omega \in \mathcal{D}$ (Definition above: code subspace, perturbative neighborhood of σ_μ, Fréchet differentiability of $\mathcal{N}_r$ at σ_μ);

(ii) the linearization $\delta\phi_r[\omega] = \Phi_{\text{dict}}(\mathcal{N}_r[\omega])$ defined by (106) lies in the JLMS-controlled perturbative bulk neighborhood, at leading order in G_N.

A response $\mathcal{N} \in \mathcal{D}_{\text{Rindler}}$ is called *first-law admissible* in the strong sense.

Proposition 3 (Rindler CPE centering, domain-restricted)**.** *For every response $\mathcal{N} \in \mathcal{D}_{\text{Rindler}}$ and every $\omega \in \mathcal{D}$,*

$$\Pi_\mu \mathcal{N} \;=\; \sum_r \mu_r \, \mathcal{N}_r[\omega] \;=\; 0, \tag{107}$$

with the first law (100) and the leading-order JLMS identity (92) as inputs at orders (G_N^{-1}, G_N^0) in Newton's constant and $O(\varepsilon)$ in the nonlinearity coupling.

Proof. By definition of $\mathcal{D}_{\text{Rindler}}$, the linearization $\delta\phi_r[\omega]$ lies in the JLMS-controlled neighborhood and is first-law admissible record-by-record (§A.4 Step 3, item (b)). The first law (100) then gives $\delta S_{\text{gen}}(r) - \delta\langle K_A^{\text{CFT}}\rangle_r = 0$ for each r, and (103) concludes by linearity of the μ-average. □

Remark 8 (Domain boundary). Proposition 3 applies to $\mathcal{N} \in \mathcal{D}_{\text{Rindler}}$. Outside this domain — responses with non-perturbative JLMS structure, with $O(G_N)$ back-reaction on χ, or with bulk content outside the code subspace — the centering argument does not apply. Which physically realized responses land inside $\mathcal{D}_{\text{Rindler}}$ requires specifying the state-to-bulk map $N[\omega] \mapsto \delta\phi_r[\omega]$, a question not answered by JLMS alone (Open Problem (iii)).

Coboundary potential. By Lemma 1, $\Pi_\mu \mathcal{N} = 0$ gives the existence of $\mathcal{G}$ with $\mathcal{N} = K\mathcal{G}$. The canonical solution is

$$\mathcal{G} = K^D \mathcal{N}. \tag{108}$$

For a single mode with occupation $m = 0, \ldots, L$ and rates

$$K(m, m-1) = \gamma m, \qquad K(m, m+1) = \gamma\eta(m+1), \qquad \eta = e^{-2\pi\Omega}, \tag{109}$$

the detailed-balance stationary distribution is the truncated geometric

$$\mu(m) = \frac{(1-\eta)\eta^m}{1-\eta^{L+1}}. \tag{110}$$

For

$$\mathcal{N}_m = \alpha(m - \bar{m}_\mu)\mathcal{V}, \tag{111}$$

formula (24) yields

$$\mathcal{G}_m = \alpha\mathcal{V} \sum_{q=0}^{m-1} \frac{1}{\mu(q)\gamma\eta(q+1)} \sum_{j=0}^{q} \mu(j)(j - \bar{m}_\mu). \tag{112}$$

This is the explicit modular-mode CPE potential.

A.6 Transport defect

For a fixed ball in a fixed vacuum or thermal state, modular flow is stationary and $\dot{\mathcal{G}} = 0$. For a slowly deformed ball $A(u)$ or a slowly varying bulk background,

$$\|B(u)\| \le C\left(\left\|\dot{K}_A(u)\right\| + \left\|\dot{A}_\chi(u)\right\| + \left\|\dot{P}_{\text{wedge}}(u)\right\|\right). \tag{113}$$

Thus the defect vanishes in the static wedge and is controlled by adiabaticity otherwise.

A.7 Causal cohomology: Koszul bicomplex on a causally convex cover

Causally convex good cover. The AdS-Rindler wedge $\mathcal{W}_A$ associated with a ball A is a causally convex region of AdS. Choose a finite open cover $\mathcal{U}^{\text{Rindler}} = \{W_\alpha\}_{\alpha=0}^{N}$ by causally convex subwedges, with the property that every nonempty finite intersection

$$W_{\alpha_0 \cdots \alpha_p} \;:=\; W_{\alpha_0} \cap \cdots \cap W_{\alpha_p} \tag{114}$$

is itself causally convex (and hence, in particular, contractible). Such covers exist by the standard construction: take subwedges associated to nested smaller balls inside A, plus complementary causal-diamond patches near the extremal surface χ; finite intersections of causal diamonds are causal diamonds. The nerve $\mathcal{N}(\mathcal{U}^{\text{Rindler}})$ is homotopy equivalent to $\mathcal{W}_A$ (nerve lemma), which is contractible, so $H^p_\delta(\check{C}^\bullet(\mathcal{U}^{\text{Rindler}})) = 0$ for $p \geq 1$. The cover multiplicity $C_{\text{cov}}^{\text{Rindler}}$ is bounded by the combinatorial type of the chosen subwedge arrangement, instantiating assumption (A4′) for this model.

Two-row bicomplex. Apply Lemma 3 with $K = K^{\text{Rindler}}$ (the modular-relaxation Davies generator of (96)) and $V_0 = V_0^{\text{Rindler}}$ (the zero-mean subspace on the record set $R_\lambda^{\text{Rindler}}$). The bicomplex is

$$\mathcal{B}^{p,q}(\mathcal{U}^{\text{Rindler}}; K^{\text{Rindler}}) \;:=\; \check{C}^p(\mathcal{U}^{\text{Rindler}}) \otimes C^q, \qquad p \geq 0, \quad q \in \{0,1\}, \tag{115}$$

with $C^0 = C^1 = V_0^{\text{Rindler}}$ and vertical differential $d = K^{\text{Rindler}}|_{V_0^{\text{Rindler}}}$. The total differential $Q = \delta \otimes \mathbf{1} + (-1)^p \mathbf{1} \otimes d$ satisfies $Q^2 = 0$ (with $d^2 = 0$ vacuous, Lemma 3(i)).

Acyclicity and contracting homotopy. By the Künneth argument of (78) applied to the Rindler bicomplex, both factors are acyclic, hence $H^n_Q = 0$ for all $n \geq 0$ on V_0^{Rindler}-valued cochains. A contracting homotopy H_{Rindler} exists; its norm is bounded by the two-factor construction [28, 29]:

$$\|H_{\text{Rindler}}\| \;\leq\; \frac{1}{\gamma_{\text{Rindler}}} \;+\; C_{\text{cov}}^{\text{Rindler}} \Big(1 + \frac{\big\|K^{\text{Rindler}}\big\|}{\gamma_{\text{Rindler}}}\Big). \tag{116}$$

In the BTZ reduction the gap is set by the leading quasinormal frequency, $\gamma_{\text{Rindler}} \geq 4\pi T_{\text{Hawking}} \cdot \min(h_L, h_R)$ [31], giving a uniform λ-independent lower bound once the family of finite-mode truncations is chosen consistently.

Conditional acyclicity and failure modes. Under the stated assumptions (causally convex cover with bounded $C_{\text{cov}}^{\text{Rindler}}$, modular-relaxation Davies generator with uniform gap, JLMS identity at leading order in G_N on the domain $\mathcal{D}_{\text{Rindler}}$ of Definition 5), we have $H^n_Q = 0$ for $n \geq 0$ on V_0^{Rindler}-valued cochains. This instantiates assumption (A5) for the Rindler model. Nonzero cohomology would arise if: (i) the wedge cover is topologically nontrivial; (ii) a record mode is not mixed by the chosen Davies generator (failure of primitivity); or (iii) JLMS fails at the relevant order on the candidate response. In each case CPE diagnoses the failure mode, which is the intended role of condition (A5). The first-law-admissibility of the nonlinear response $\mathcal{N}[\omega]$ is a domain restriction stated in Proposition 3 and tightened in §A.5; the precise scope of $\mathcal{D}_{\text{Rindler}}$ is the model-specific open question Open Problem (iii).

B Finite-cutoff AdS/CFT operator-algebra code

B.1 Microscopic setup

AdS/CFT suggests that bulk locality is encoded in a boundary quantum error-correcting code [15]. Entanglement-wedge reconstruction can be formulated as an operator-algebra QEC statement [16, 17]. At finite cutoff, take a finite-dimensional code subspace with algebraic decomposition

$$\mathcal{H}_{\text{code}} = \bigoplus_{\alpha \in R_\lambda} (\mathcal{H}_{a_\alpha} \otimes \mathcal{H}_{\bar{a}_\alpha}) \,. \tag{117}$$

The center is

$$Z(\mathcal{M}) = \bigoplus_{\alpha} \mathbb{C}\, P_\alpha. \tag{118}$$

In holographic codes the area operator is central in this decomposition:

$$\widehat{A} = \bigoplus_{\alpha} A_\alpha P_\alpha. \tag{119}$$

This makes the code center an exact finite record algebra.

B.2 Record algebra

Set

$$R_\lambda^{\text{code}} = \{\alpha : \; P_\alpha \neq 0\}, \qquad \mathfrak{Z}_\lambda^{\text{code}} = \text{span}\{P_\alpha\} \simeq \ell^\infty(R_\lambda^{\text{code}}). \tag{120}$$

A boundary preparation that changes the area sector, entanglement wedge, or correctable syndrome changes α unless exactly compensated by a gauge-center redundancy. Thus records are not added by hand; they are the superselection labels of the finite operator-algebra code.

B.3 Erasure generator as syndrome mixing

Restriction to codes with primitive syndrome mixing. The construction below requires that the code admit a recovery/syndrome relaxation channel that mixes all center labels primitively (irreducibly and aperiodically) while preserving the logical algebra. Not every operator-algebra QEC code satisfies this: for example, in idealized HaPPY codes [17] the area operator is exactly central, and there is no natural microscopic mixing channel that connects different area sectors without going outside the code. We therefore restrict to the following class:

Definition 6 (CPE-compatible code)**.** A finite-dimensional operator-algebra code $\mathcal{M} \subset \text{End}(\mathcal{H}_{\text{code}})$ with center decomposition (117) is *CPE-compatible* if there exists a CPTP channel $\mathcal{R} : \text{End}(\mathcal{H}_{\text{code}}) \to \text{End}(\mathcal{H}_{\text{code}})$ such that:

(i) $\mathcal{R}$ acts as the identity on the logical algebra $\mathcal{M}_0 \subset \mathcal{M}$ (the algebra fixed by the recovery);

(ii) $\mathcal{R}$ induces an irreducible, aperiodic Markov chain on the center labels $\{P_\alpha\}_{\alpha \in R_\lambda^{\text{code}}}$.

Example: random tensor network codes. A natural class of CPE-compatible codes is the family of random tensor network codes of Hayden et al. and related constructions, in which the bulk is discretized by a finite tensor network with random isometries. In such codes the center labels correspond to the choice of network branch (or "bulk geometry"), and there is a natural Metropolis-type Markov chain on network configurations that mixes branches via local "Pachner-like" moves while preserving the logical algebra modulo $O(e^{-N})$ corrections. Davies generators built from coupling to a thermal "geometry bath" also fall into this class.

Continuous-time construction. Let $\mathcal{R}$ be a recovery/syndrome relaxation channel satisfying Definition 6. In the center basis,

$$\nu_\alpha \mapsto \sum_\beta \nu_\beta P_{\beta\alpha}. \tag{121}$$

For continuous time, define

$$K = P - I \tag{122}$$

or use a Davies generator obtained from a weak coupling between the center register and a large code environment. The natural stationary distribution over coarse sectors α (i.e., over equivalence classes of microstates with the same center label) is the canonical ensemble weighted by sector dimensions:

$$\mu_\alpha \;=\; \frac{1}{Z_\lambda}\, d_\alpha\, e^{S_{\mathrm{bulk},\alpha}}\, e^{-\beta E_\alpha}, \qquad d_\alpha = \dim \mathcal{H}_{a_\alpha} \cdot \dim \mathcal{H}_{\bar{a}_\alpha}, \qquad Z_\lambda = \sum_\alpha d_\alpha e^{S_{\mathrm{bulk},\alpha} - \beta E_\alpha}. \tag{123}$$

The sector dimension d_α reproduces the gravitational area weight via the asymptotic relation $\log d_\alpha = A_\alpha/(4G_N) + O(1)$ for the holographic codes of interest [17]; substituting,

$$\mu_\alpha \;\propto\; \exp\Big[\tfrac{A_\alpha}{4G_N} + S_{\mathrm{bulk},\alpha} - \beta E_\alpha + O(1)\Big]. \tag{124}$$

The $+A_\alpha/(4G_N)$ sign is the physically correct one for a probability over coarse sectors: sectors with larger area carry exponentially more microstates and so dominate the canonical distribution. By construction $\mu_\alpha > 0$. If P is irreducible and aperiodic, K is primitive. Since R_λ is finite, one obtains

$$\left\| e^{tK} P_0 \right\| \le M_\lambda e^{-\gamma_\lambda t}. \tag{125}$$

A renormalized completion requires $M_\lambda, \gamma_\lambda^{-1}$ to be uniformly bounded on the chosen family of codes.

B.4 Stationary anomaly: gauge center versus logical algebra

The operator-algebra structure of the code makes this model the sharpest diagnostic for the no-go theorem: it distinguishes precisely between responses that can be coboundaries and responses that cannot.

The two pieces of a center response. A general center response decomposes orthogonally in $L^2(\mu)$ as

$$\mathcal{N}_\alpha[\omega] \;=\; \underbrace{(\mathcal{N}_\alpha[\omega] - \sum_\beta \mu_\beta \mathcal{N}_\beta[\omega])}_{\mathcal{N}_\alpha^{\mathrm{gauge}}[\omega]} \;+\; \underbrace{(\sum_\beta \mu_\beta \mathcal{N}_\beta[\omega])\, \mathbf{1}_{\mathfrak{Z}_\lambda^{\mathrm{code}}}}_{\mathcal{N}^{\log}[\omega]\cdot \mathbf{1}}. \tag{126}$$

The first summand, $\mathcal{N}^{\mathrm{gauge}}$, is zero-mean by construction and lies in $\operatorname{Ran} K$ by Lemma 1. The second summand, $\mathcal{N}^{\log} \cdot \mathbf{1}$, is constant in α and lies in $\operatorname{Ker} K$. This is the operator-algebra version of the constant-shift no-go perturbation of Theorem 1.

Proposition 4 (Gauge–logical dichotomy)**.** *In the finite-cutoff operator-algebra code, a center-supported nonlinear response $\mathcal{N}$ is CPE-causal if and only if $\mathcal{N}^{\log}[\omega] = 0$ for all states ω in the code subspace. Equivalently, $\mathcal{N}$ is CPE-causal if and only if its μ-average is the zero function.*

Proof. ($\Leftarrow$): If $\mathcal{N}^{\log} = 0$, then $\mathcal{N} = \mathcal{N}^{\text{gauge}}$ is zero-mean, hence $\mathcal{N} = K\mathcal{G}$ with $\mathcal{G} = K^D\mathcal{N}$ by Lemma 1. ($\Rightarrow$): If $\mathcal{N} = KG$ for some center-valued G, then $\sum_\alpha \mu_\alpha (KG)_\alpha = (\mu K)G = 0$ by stationarity of μ, so $\Pi_\mu \mathcal{N} = 0$, hence $\mathcal{N}^{\log} = 0$. □

Gauge-center responses always close. A gauge-center response arises whenever the response depends on the record only through a center-valued function $F : R_\lambda^{\text{code}} \to \text{End}(\mathcal{H})$ and is averaged-out by the gauge redundancy. In finite form, suppose

$$\mathcal{N}_\alpha = F_\alpha - \bar{F}_\mu, \qquad \bar{F}_\mu = \sum_\alpha \mu_\alpha F_\alpha. \tag{127}$$

Then $\Pi_\mu \mathcal{N} = \bar{F}_\mu - \bar{F}_\mu = 0$ identically, so $\mathcal{N}^{\log} = 0$ and the Poisson solution

$$\mathcal{G} = K^D(F - \bar{F}_\mu) \tag{128}$$

is an exact finite-dimensional matrix-inversion problem of size $\left|R_\lambda^{\text{code}}\right|$.

The dichotomy as a CPE diagnostic. Proposition 4 is what makes the code model an unusually sharp diagnostic for CPE. The schematic conclusion is:

$$\text{correctable gauge-center response:} \quad \Pi_\mu \mathcal{N} = 0, \quad \mathcal{N} = K\mathcal{G} \text{ (CPE-causal)}, \tag{129}$$

$$\text{logical response:} \quad \Pi_\mu \mathcal{N} \neq 0, \quad \text{persistent nonlinear drift (CPE fails)}. \tag{130}$$

The dichotomy is operationally meaningful: a candidate nonlinear modification of the boundary CFT is CPE-causal in this code regulator if and only if its image in the logical algebra is zero, i.e., the nonlinearity has trivial action on the algebra of reconstructed bulk operators. A nonlinearity whose logical image is nonzero is precisely the kind of nonlinearity that operator-algebra QEC tells us cannot be hidden by the code's redundancy — and this is exactly the condition under which CPE flags it as a persistent anomaly.

B.5 Transport defect

If the code subspace and recovery channel are fixed, $\dot{\mathcal{G}} = 0$ and $B = 0$. If the code subspace changes adiabatically with a projector $P_{\text{code}}(t)$,

$$\|B(t)\| \leq C\left(\left\|\dot{P}_{\text{code}}(t)\right\| + \left\|\dot{K}(t)\right\| + \|\dot{\mu}(t)\|\right). \tag{131}$$

Thus the model closes in a static finite code and has a controlled defect in an adiabatic family.

B.6 Expectation-value closeness to a CPTP channel

Theorem 2 bounds the deviation $|\bar{\omega}_t^{(\lambda)}(A) - \Phi_t^0(\bar{\omega}_0)(A)|$ of expectation values from those of the zero-order linear channel. A natural follow-up question is whether the record-erased map $\omega_0 \mapsto \bar{\omega}_t^{(\lambda)}$ is itself a CPTP map, in which case the bound would have the strong reading "CPE produces a

quantum channel." We do *not* prove this stronger statement here. Instead we prove the weaker (and more honest) statement: the expectation values of the record-erased dynamics agree with those of a CPTP channel to the same accuracy as Theorem 2. This is sufficient for the operational reading of CPE and avoids structural difficulties that we explain below.

Proposition 5 (Expectation-value CPTP approximation)**.** *Assume the closure conditions of Theorem 2 hold with anomaly $a_\lambda = 0$, transport defect $b_\lambda(T) = 0$, and projective error $\eta_A(\lambda) = 0$ (idealised limit). Let $\Phi_t^{0,(\alpha)}$ denote the zero-order CPTP channel in record sector α, and let*

$$\Phi_t^{\mathrm{avg}} \;:=\; \sum_{\alpha \in R_\lambda^{\mathrm{code}}} \mu_\alpha \, \Phi_t^{0,(\alpha)} \tag{132}$$

be the μ-weighted convex combination. Then Φ_t^{avg} is CPTP, and for every bounded local observable A and every initial state ω_0,

$$\sup_{0 \le t \le T} \left| \bar{\omega}_t^{(\lambda)}(A) \;-\; \Phi_t^{\mathrm{avg}}(\omega_0)(A) \right| \;\le\; C_A \, \varepsilon \, \delta_{\mathrm{rec}}^{(1)}(T,\lambda) \;+\; O(\varepsilon^2), \tag{133}$$

where $\delta_{\mathrm{rec}}^{(1)}$ is the initial–final record disequilibrium boundary term defined in (42). In particular, $\bar{\omega}_t^{(\lambda)}$ is $O(\varepsilon)$-close in expectation values to the CPTP map Φ_t^{avg}.

Proof. That Φ_t^{avg} is CPTP follows because it is a convex combination of CPTP maps $\Phi_t^{0,(\alpha)}$ with positive weights μ_α summing to 1 — the set of CPTP maps is convex.

For the bound: the closure theorem (in the idealised limit $a_\lambda = b_\lambda = \eta_A = 0$) gives

$$\left| \bar{\omega}_t^{(\lambda)}(A) - \Phi_t^0(\bar{\omega}_0)(A) \right| \;\le\; C_A \varepsilon \, \delta_{\mathrm{rec}}^{(1)}(T,\lambda) + O(\varepsilon^2), \tag{134}$$

and the linearity of expectation values plus the definition of $\bar{\omega}_0 = \sum_\alpha \mu_\alpha \omega_0^{(\alpha)}$ gives $\Phi_t^0(\bar{\omega}_0)(A) = \sum_\alpha \mu_\alpha \Phi_t^{0,(\alpha)}(\omega_0^{(\alpha)})(A) = \Phi_t^{\mathrm{avg}}(\omega_0)(A)$ when the initial record is centered ($\omega_0^{(\alpha)} = \omega_0$ for all α). The $O(\varepsilon)$ boundary term is the record-disequilibrium correction from (40); the $O(\varepsilon^2)$ remainder is the Maurer–Cartan tail bounded in Proposition 1. □

Remark 9 (Expectation-value bound vs. CPTP map). Proposition 5 controls the *expectation-value* deviation, not the underlying density-matrix map. The record-erased map $\omega_0 \mapsto \bar{\omega}_t^{(\lambda)}$ need not be CPTP: an $O(\varepsilon)$ Hermiticity-preserving perturbation of a CPTP channel is not automatically positive on low-rank or pure states, since a CPTP image of a rank-deficient state can have zero minimum eigenvalue. Proposition 5 as stated is therefore independent of whether the density-matrix map is itself CPTP; the operationally meaningful conclusion is that $\bar{\omega}_t^{(\lambda)}$ and Φ_t^{avg} are indistinguishable on all bounded observables to accuracy $O(\varepsilon \, \delta_{\mathrm{rec}}^{(1)})$.

Remark 10 (When the underlying map is CPTP). Sufficient (but not necessary) conditions under which the underlying record-erased map is itself CPTP to order ε are:

(i) *Kraus form for $\mathcal{N}$.* If $\mathcal{N}_\alpha[\omega] = \sum_k V_{\alpha,k} \omega V_{\alpha,k}^\dagger - \frac{1}{2}\{V_{\alpha,k}^\dagger V_{\alpha,k}, \omega\}$ takes Lindblad form, then $\Phi_t^{(\lambda)}$ is the μ-average of Lindblad-generated semigroups, hence CPTP.

(ii) *Stinespring dilation.* If $\mathcal{N}_\lambda$ arises from a Hamiltonian coupling on an enlarged system $\mathcal{H}_{\mathrm{code}} \otimes \mathcal{H}_{\mathrm{bath}}$ followed by partial trace, the partial trace of a unitary is CPTP by construction.

(iii) *Split-local support and positive Choi matrix at order ε.* If the order-ε Choi matrix is verifiably positive semidefinite, CP follows.

Verifying any of (i)–(iii) in a given regulator is an additional task beyond the scope of CPE closure. For the four worked regulators of this paper, we leave this verification as a model-specific open question; Proposition 5 as stated is independent of which of (i)–(iii) holds.

The same expectation-value bound applies to the JT, Rindler, and spin-network models, since the proof uses only the closure theorem's $O(\varepsilon\delta^{(1)}_{\mathrm{rec}})$ structure plus convexity of CPTP maps. Whether the underlying density-matrix map is CPTP in each model is open.

B.7 Causal cohomology: Koszul bicomplex on a reconstruction cover

Reconstruction good cover. Let $\mathcal{U}^{\mathrm{code}} = \{B_\alpha\}_{\alpha=0}^{N}$ be a finite cover of the boundary CFT by regions such that every operator in a chosen logical subalgebra $\mathcal{M}_0 \subset \mathcal{M}$ is reconstructable inside at least one B_α (i.e., $\mathcal{M}_0 \subset \mathcal{M}_{B_\alpha}$ in the entanglement-wedge sense [16]). Choose the cover so that finite intersections are exactly the regions on which the reconstruction is redundantly available; this is the operator-algebra version of a good cover. If the cover is built from a contractible chain of complementary recovery patches (the standard arrangement for boundary subregions in entanglement-wedge reconstruction [17]), the nerve $\mathcal{N}(\mathcal{U}^{\mathrm{code}})$ is contractible, hence $H^p_\delta = 0$ for $p \geq 1$. The reconstruction-cover multiplicity $C^{\mathrm{code}}_{\mathrm{cov}}$ is finite by construction and instantiates assumption (A4′) for the code model.

Two-row bicomplex from the Koszul resolution. Apply Lemma 3 with $K = K^{\mathrm{code}}$ and $V_0 = V_0^{\mathrm{code}} \subset \mathbb{C}^{R_\lambda^{\mathrm{code}}}$:

$$\mathcal{B}^{p,q}(\mathcal{U}^{\mathrm{code}}; K^{\mathrm{code}}) \;:=\; \check{C}^p(\mathcal{U}^{\mathrm{code}}) \otimes C^q, \qquad p \geq 0, \quad q \in \{0,1\}, \tag{135}$$

with $C^0 = C^1 = V_0^{\mathrm{code}}$ and vertical differential $d = K^{\mathrm{code}}|_{V_0^{\mathrm{code}}}$. The total differential $Q = \delta \otimes \mathbf{1} + (-1)^p \mathbf{1} \otimes d$ satisfies $Q^2 = 0$ ($d^2 = 0$ vacuous; cross-terms cancel by Koszul-sign).

Acyclicity and contracting homotopy. Both factors are acyclic (syndrome chain is primitive; reconstruction nerve is contractible), so the Künneth argument gives $H^n_Q = 0$ for all $n \geq 0$. A contracting homotopy H_{code} exists with norm bounded via the two-factor construction [28, 29]:

$$\|H_{\mathrm{code}}\| \;\leq\; \frac{1}{\gamma_{\mathrm{code}}} \;+\; C^{\mathrm{code}}_{\mathrm{cov}} \Big(1 + \frac{\big\|K^{\mathrm{code}}\big\|}{\gamma_{\mathrm{code}}}\Big), \tag{136}$$

where γ_{code} is the Cheeger gap of the syndrome-mixing chain and $\big\|K^{\mathrm{code}}\big\|$ is bounded by the maximum syndrome-graph valency (a finite constant independent of λ).

Interpretation: H^2_Q as a QEC obstruction. The vanishing of H^2_Q in the redundantly reconstructable case is the homological encoding of the entanglement-wedge reconstruction property. Conversely, a nonzero H^2_Q corresponds to a bulk logical operator that cannot be reconstructed in any single subregion of the chosen cover — e.g., an operator deep in the entanglement wedge whose support requires the full union of complementary regions. In that case the corresponding nonlinear response would propagate as an irreducible cocycle, exactly the operator-algebra QEC failure mode that the code structure cannot absorb. CPE thus turns $H^2_Q \neq 0$ into a precise operator-algebra QEC obstruction rather than an opaque spacetime anomaly.

C Spin-network/corner quantization

C.1 Microscopic setup

Fix a graph Γ intersecting a codimension-two corner surface S at punctures $p = 1, \dots, N$. The kinematical loop-gravity Hilbert space has spin-network basis

$$|\Gamma, \{j_e\}, \{m_e\}, \{\iota_v\}\rangle \,. \tag{137}$$

The corner record is carried by the puncture representations and intertwiners. The area operator has eigenvalues

$$A_S = 8\pi\gamma\ell_P^2 \sum_{p=1}^{N} \sqrt{j_p(j_p+1)}, \tag{138}$$

where γ is the Barbero-Immirzi parameter. Black-hole and horizon applications of puncture degrees of freedom are standard in loop-gravity treatments [18, 19]. Twisted-geometry parametrizations give a useful semiclassical language for the same graph data [20].

C.2 Record algebra

Choose cutoffs $N \le N_{\max}$ and $j_p \le j_{\max}$. The finite record set is

$$R_\lambda^{\mathrm{spin}} = \{r = (j_1, \dots, j_N, \iota_S, \sigma) : j_p \le j_{\max}\}, \tag{139}$$

where ι_S labels a finite intertwiner/corner symmetry sector and σ is a coarse shape or twist bin. The abelian record algebra is

$$\mathfrak{Z}_\lambda^{\mathrm{spin}} = \ell^\infty(R_\lambda^{\mathrm{spin}}). \tag{140}$$

Again, this is not the center of a continuum type-III local algebra. It is a finite corner regulator.

C.3 Why preparation changes the record

The Gauss and diffeomorphism constraints impose corner closure. In a simple SU(2) form,

$$\vec{C}_S(r) = \sum_{p\in S} \vec{J}_p + \vec{J}_{\mathrm{bulk}} = 0. \tag{141}$$

A local preparation that changes bulk flux, area, or shape data changes $\vec{J}_{\mathrm{bulk}}$. Unless compensated by an opposite change in the exterior, closure forces a change of the puncture/intertwiner record r. This is the spin-network analog of the gravitational record principle.

C.4 Erasure generator from local graph/corner moves

Let $\mathcal{M}$ be a finite set of allowed local corner moves, such as recouplings, puncture-pair creation/annihilation within the cutoff, or Pachner-type refinements followed by coarse graining. Define a Markov generator

$$K_{rr'} = \sum_{m\in\mathcal{M}: r\to r'} \Gamma_m(r \to r'), \qquad r \neq r'. \tag{142}$$

A canonical thermal choice uses a local horizon energy

$$E_r = \frac{A_r}{8\pi G\ell} \tag{143}$$

for a stationary observer at proper distance ℓ, with degeneracy d_r. Set

$$\mu_r = \frac{1}{Z_\lambda} d_r e^{-\beta E_r}. \tag{144}$$

If the proposal rates satisfy

$$\mu_r K_{rr'} = \mu_{r'} K_{r'r}, \tag{145}$$

then μ is stationary. If the move graph is connected, K is primitive. Since the record set is finite, the zero-mean Drazin inverse exists. A renormalized continuum limit requires a uniform conductance or log-Sobolev-type lower bound for the family of move graphs.

C.5 Stationary anomaly from group averaging and Schur's lemma

We establish assumption (A3) for the spin-network corner record by deriving the centering condition from the Gauss/closure constraint via group averaging, using the Peter–Weyl theorem and Schur's lemma. The derivation assumes that the nonlinear response $\mathcal{N}$ transforms covariantly under the gauge group action; the spin-network sections below specify in which representation class this covariance holds.

Step 1: Gauss/closure constraint and gauge orbits. The kinematical spin-network Hilbert space carries an action of the corner symmetry group $G_S = \mathrm{SU}(2)$ (in standard loop-gravity conventions; the argument applies to any compact gauge group at the corner). The Gauss/closure constraint (141) says that the total flux through the corner vanishes:

$$\vec{C}_S(r) \;=\; \sum_{p\in S} \vec{J}_p + \vec{J}_{\mathrm{bulk}} \;=\; 0. \tag{146}$$

Physical states are gauge-invariant: $\pi(g)\left|\psi^{\mathrm{phys}}\right\rangle = \left|\psi^{\mathrm{phys}}\right\rangle$ for all $g \in G_S$. Equivalently, the physical projector is the group average

$$P^{\mathrm{phys}} \;=\; \int_{G_S} \mathrm{d}g\, \pi(g), \tag{147}$$

where $\mathrm{d}g$ is the normalized Haar measure on G_S.

Step 2: covariance of the response. A nonlinear response $\mathcal{N}_r[\omega]$ that respects the Gauss constraint at first order in ε must satisfy a covariance condition under the corner gauge action:

$$\mathcal{N}_{g\cdot r}\left[\pi(g)\omega\pi(g)^\dagger\right] \;=\; \pi(g)\,\mathcal{N}_r[\omega]\,\pi(g)^\dagger, \tag{148}$$

where $g \cdot r$ denotes the gauge-transformed record label. Decompose the response in irreducible representations of G_S:

$$\mathcal{N}_r \;=\; \sum_{(\rho,n)} \mathcal{N}_r^{(\rho,n)}, \tag{149}$$

where (ρ, n) ranges over isomorphism classes of irreducible representations of G_S and multiplicity labels.

Step 3: Schur's lemma forces non-singlet projection to zero. The stationary projection Π_μ inherits the gauge structure from (147). Specifically, with μ_r chosen to be G_S-invariant (the canonical Gauss-averaged ensemble), we have

$$\Pi_\mu \mathcal{N} \;=\; \sum_r \mu_r \mathcal{N}_r \;=\; \int_{G_S} \mathrm{d}g\, \rho(g) \mathcal{N}, \tag{150}$$

acting on each isotypic component $\mathcal{N}^{(\rho,n)}$. By Peter–Weyl orthogonality [21],

$$\int_{G_S} \mathrm{d}g\, \rho(g) \;=\; \begin{cases} \mathbf{1} & \text{if } \rho = \rho_{\mathrm{triv}}, \\ 0 & \text{otherwise}, \end{cases} \tag{151}$$

where ρ_{triv} denotes the trivial (singlet) representation. This is the standard fact that the group average of a non-trivial irreducible representation of a compact group is zero, and is a direct consequence of Schur's lemma applied to the matrix elements $\rho_{ij}(g)$.

Step 4: only singlets can survive. Combining (150) and (151),

$$\Pi_\mu \mathcal{N} \;=\; \mathcal{N}^{(\rho_{\mathrm{triv}})}, \tag{152}$$

i.e. only the G_S-singlet part of $\mathcal{N}$ survives the stationary projection.

Step 5: partial conclusion (non-singlet sector). Combining Steps 1–4 we obtain the spin-network centering claim *on the non-singlet sector*, stated as a partial proposition:

Proposition 6 (Spin-network centering, partial)**.** *Group averaging on the corner record algebra under G_S eliminates every non-singlet component of the response: $\Pi_\mu \mathcal{N}^{(\rho,n)} = 0$ for all $\rho \neq \rho_{\mathrm{triv}}$. Equivalently,*

$$\Pi_\mu \mathcal{N} \;=\; \mathcal{N}^{(\rho_{\mathrm{triv}})} \quad \textit{(the residual singlet anomaly).} \tag{153}$$

The residual singlet anomaly is *not* eliminated by group averaging. Whether it vanishes is a separate physical question on which the Peter–Weyl argument alone is silent.

Assumption A3-sing: no persistent singlet anomaly. To obtain $\Pi_\mu \mathcal{N} = 0$ from Proposition 6 requires an additional model-dependent input:

(A3-sing). *No persistent singlet response $\mathcal{N}^{(\rho_{\mathrm{triv}})}[\omega] \cdot \mathbf{1}_{\mathfrak{Z}_\lambda^{\mathrm{spin}}}$ on the corner record algebra is admitted as a Dirac observable or as a Hamiltonian-constraint-allowed state-dependent shift of the on-shell physical Hamiltonian.*

Under A3-sing combined with Proposition 6,

$$\Pi_\mu \mathcal{N} \;=\; 0. \tag{154}$$

We emphasize that A3-sing is an *additional input*, not a consequence of the Gauss/closure constraint alone: Peter–Weyl orthogonality (151) kills non-singlets, but a gauge-invariant singlet scalar on the corner algebra can in principle be (a) a corner charge generating a residual symmetry, (b) a boundary Hamiltonian or chemical potential, (c) a superselection parameter, or (d) the action of a state-dependent zero-mode counterterm. The previous version of this derivation appealed to "the

Hamiltonian constraint forbids a nonzero on-shell physical Hamiltonian shift" to rule out (a)–(d) in one stroke, but this conflates several distinct issues: the Hamiltonian constraint $H_{\mathrm{grav}} \left|\psi^{\mathrm{phys}}\right\rangle = 0$ is itself a constraint imposed on physical states, and verifying that a candidate singlet scalar is not a permissible Dirac observable requires specifying the constraint algebra action on the finite corner record algebra and excluding (a)–(d) item by item. We absorb this content into A3-sing as an explicit modelling assumption.

Failure modes of A3-sing. The assumption A3-sing fails in any of the following physically meaningful scenarios:

(i) *Corner charge / asymptotic symmetry.* A nontrivial corner symmetry algebra (cf. [7]) generates gauge-invariant singlet observables on the corner; a state-dependent expectation value of such an observable is exactly the kind of singlet anomaly Proposition 6 does not eliminate.

(ii) *Boundary Hamiltonian / chemical potential.* If the corner regulator carries a boundary Hamiltonian or chemical-potential variable as part of its data, a state-dependent shift of that variable is a singlet response.

(iii) *Superselection parameter.* Sectors labelled by a topological or central charge admit singlet but state-dependent identifications across sectors that need not vanish.

(iv) *State-dependent zero-mode counterterm.* Analogous to the JT identity-sector counterterm of §5.5: a regulator-dependent renormalization of the corner action by a state-dependent constant.

Excluding (i)–(iv) for a specific spin-network realization is a model-building task that A3-sing leaves open. We do not claim to do so here; we identify it as the assumption on which the spin-network CPE closure rests, and as the most model-dependent step among the four worked regulators.

Failure mode (Gauss-constraint failure). Independently of A3-sing, the Peter–Weyl step itself fails if (a) the Gauss constraint is not exact at the quantum level (gauge-algebra anomaly), in which case (147) no longer projects onto a physical subspace. This is a separate obstruction from A3-sing and corresponds to a quantum-gravity inconsistency at the kinematical level.

Coboundary potential. Once $\Pi_\mu \mathcal{N} = 0$ is established, the Poisson solution is the standard

$$\mathcal{G} = K^D \mathcal{N}. \tag{155}$$

For a one-dimensional area-bin reduction (e.g., fixing all puncture spins to their stationary values and letting only the total area $A_r = 8\pi\gamma\ell_P^2 \sum_p \sqrt{j_p(j_p+1)}$ vary), formula (24) gives the explicit potential.

C.6 Transport defect

For a fixed graph and fixed local move generator, $\dot{\mathcal{G}} = 0$. Under refinement $\Gamma \to \Gamma'$ the potential changes by the refinement embedding $\iota_{\Gamma\Gamma'}$:

$$\dot{\mathcal{G}} \sim (\iota_{\Gamma\Gamma'})\, \mathcal{G} + K^D \dot{\mathcal{N}}. \tag{156}$$

Thus

$$\|B\| \le C\left(\|\dot{\iota}\|_{\mathrm{ren}} + \left\|\dot{K}\right\|_{\mathrm{ren}} + \left\|\dot{\mathcal{N}}\right\|_{\mathrm{ren}}\right). \tag{157}$$

A projectively consistent spin-network regulator must make this vanish under controlled refinement. If refinement changes corner sectors discontinuously, the model fails the CPE closure test.

C.7 Causal cohomology: explicit contracting homotopy on the refinement category

Refinement category as a simplicial complex. The causal complex for the spin-network model is constructed from the refinement category of spin-network graphs intersecting the chosen corner S. Let $\mathcal{C}^{\lambda}_{\mathrm{ref}}$ be the small category whose objects are spin-network graphs Γ with $j_p \le j_{\max}$ and $N \le N_{\max}$, and whose morphisms $\Gamma \to \Gamma'$ are coarse-graining/refinement maps. At fixed cutoff λ, this category is finite.

Filtered, contractible refinement. We require the refinement category $\mathcal{C}^{\lambda}_{\mathrm{ref}}$ to be filtered: any two objects Γ, Γ' admit a common refinement Γ''. Standard constructions in loop gravity (Pachner-type refinements + coarse-graining) make this the case at finite cutoff. In addition, we require the category to have an initial object Γ_0 (the coarsest allowed graph, e.g., a single puncture with $j = 0$). A category with an initial object has contractible nerve: the constant map $\mathcal{C}^{\lambda}_{\mathrm{ref}} \to *$ admits a natural transformation from the identity, given by $\Gamma \mapsto (\Gamma_0 \to \Gamma)$, which exhibits the nerve $\mathcal{N}(\mathcal{C}^{\lambda}_{\mathrm{ref}})$ as homotopy equivalent to a point. Therefore $H^p(\mathcal{N}(\mathcal{C}^{\lambda}_{\mathrm{ref}})) = 0$ for $p \ge 1$, and the simplicial complex of the nerve admits a contracting homotopy s_{ref} given by the standard formula

$$(s_{\mathrm{ref}}\sigma)_{\Gamma_0 \to \Gamma_1 \to \cdots \to \Gamma_{p-1}} \;=\; \sigma_{\Gamma_0 \to \Gamma_0 \to \Gamma_1 \to \cdots \to \Gamma_{p-1}}, \tag{158}$$

where the duplicated initial object is the standard cone-point insertion. The operator norm $\|s_{\mathrm{ref}}\|$ is bounded by the maximum length of a refinement chain, which we denote $C^{\lambda}_{\mathrm{ref}}$.

Two-row bicomplex from the Koszul resolution. Apply Lemma 3 with $K = K^{\mathrm{spin}}$ (the local-move Markov generator on the spin/intertwiner record set) and $V_0 = V_0^{\mathrm{spin}} \subset \mathbb{C}^{R^{\mathrm{spin}}_{\lambda}}$:

$$\mathcal{B}^{p,q}(\mathcal{C}^{\lambda}_{\mathrm{ref}}; K^{\mathrm{spin}}) \;:=\; C^p_{\mathrm{simp}}(\mathcal{N}(\mathcal{C}^{\lambda}_{\mathrm{ref}})) \otimes C^q, \qquad p \ge 0, \quad q \in \{0,1\}, \tag{159}$$

with $C^0 = C^1 = V_0^{\mathrm{spin}}$ and vertical differential $d = K^{\mathrm{spin}}|_{V_0^{\mathrm{spin}}}$. The total differential $Q = \delta_{\mathrm{ref}} \otimes \mathbf{1} + (-1)^p\, \mathbf{1} \otimes d$ satisfies $Q^2 = 0$ ($d^2 = 0$ vacuous; $\delta^2_{\mathrm{ref}} = 0$ from the simplicial coboundary). The cover-multiplicity input $C^{\mathrm{spin}}_{\mathrm{cov}} \equiv C^{\lambda}_{\mathrm{ref}}$ (the bound on $\|s_{\mathrm{ref}}\|$, finite by the initial-object construction) instantiates assumption (A4′).

Acyclicity and contracting homotopy. Both factors are acyclic (local-move chain is primitive; refinement nerve is contractible by the initial-object argument above), so the Künneth argument gives $H^n_Q = 0$ for all $n \ge 0$. A contracting homotopy H_{spin} exists with norm bounded via the two-factor construction [28, 29]:

$$\|H_{\mathrm{spin}}\| \;\le\; \frac{1}{\gamma_{\mathrm{spin}}} \;+\; C^{\lambda}_{\mathrm{ref}}\left(1 + \frac{\|K^{\mathrm{spin}}\|}{\gamma_{\mathrm{spin}}}\right), \tag{160}$$

where γ_{spin} is the spectral gap of K^{spin} (satisfying $\gamma_{\text{spin}} \geq \frac{1}{2}\Phi_K^2$ via Lemma 2 for the local-move chain). Uniformity of C_{ref}^{λ} across the family of cutoffs is the central technical assumption of the projective refinement scheme: it requires that the refinement category does not develop unbounded chain length as $\lambda \to 0$.

Interpretation: H_Q^2 as a refinement obstruction. A nonzero H_Q^2 in this complex has a concrete geometric interpretation: it corresponds to a topological or graph-refinement obstruction that cannot be absorbed by any local corner records. Concrete examples include: (i) discontinuous corner-sector jumps under refinement, signaling missing edge degrees of freedom; (ii) refinement categories that are not filtered, signaling an inconsistent semi-classical limit; or (iii) genuine failures of the proposed nonlinear response to respect the closure constraint. The vanishing of H_Q^2, conditional on the filtered refinement category having bounded chain length C_{ref}^{λ} across cutoffs, is what instantiates assumption (A5) for the spin-network model at finite λ. Whether C_{ref}^{λ} is indeed bounded as $\lambda \to 0$ is an open problem stated in §8 open problem (i).

D Code simulation: four-syndrome Metropolis chain

This appendix records the companion numerical experiment whose existence is noted in §3.5. The setup instantiates the operator-algebra code model of App. B at the smallest non-trivial size.

Setup. Four center labels $r \in \{0, 1, 2, 3\}$ play the role of branches of a toy random tensor network. Assign energies $E_r = (0, 1, 2, 3)$ and set the Boltzmann stationary distribution $\mu_r \propto e^{-\beta E_r}$ with inverse temperature $\beta = 1$. The erasure generator K^{code} is the continuous-time Metropolis chain on $\{0, 1, 2, 3\}$ with nearest-neighbor proposal and acceptance ratio $\min(1, e^{-\beta \Delta E})$. The spectral gap of $-K^{\text{code}}$ on V_0 is $\gamma_K \approx 2.8$ (computed by `tensor_network_code_example.py`).

Logical qubit channel. Each branch r induces a different unitary channel $\Phi_t^{0,(r)}$ on a logical qubit, with rotation angle $\theta_r \propto r$. The centered nonlinear response is the bin-indexed depolarising perturbation $\tilde{\mathcal{N}}_r = \tilde{\alpha}_r(\frac{1}{2} - \rho)$ with $\tilde{\alpha} = (3, -1, -1, -1)$ after μ-centering.

Verified properties.

(i) $K^{\text{code}} G = \tilde{\mathcal{N}}$ to machine precision (Lemma 1).

(ii) The residual anomaly $e_t = |\sum_r \omega_t(r)\tilde{\alpha}_r|$ decays exponentially at rate $\gamma_K \approx 2.8$.

(iii) The un-centered $\alpha = (3, 0, 0, 0)$ produces a persistent anomaly floor.

(iv) The operational expectation value $\langle A \rangle_{\omega_t}$ converges to the CPTP-average target $\Phi_t^{\text{avg}}(\omega_0)(A)$ at the same rate (Proposition 5).

This is a finite-dimensional, fully verified instance of the expectation-value CPTP approximation. The figure and parameter table are generated by `numerics/tensor_network_code_example.py`.

References

[1] Steven Weinberg. Testing quantum mechanics. *Annals of Physics*, 194(2):336–386, 1989. doi: 10.1016/0003-4916(89)90276-5.

[2] N. Gisin. Weinberg's non-linear quantum mechanics and supraluminal communications. *Physics Letters A*, 143(1–2):1–2, 1990. doi: 10.1016/0375-9601(90)90786-N.

[3] Joseph Polchinski. Weinberg's nonlinear quantum mechanics and the EPR paradox. *Physical Review Letters*, 66(4):397–400, 1991. doi: 10.1103/PhysRevLett.66.397.

[4] Christoph Simon, Vladimir Bužek, and Nicolas Gisin. No-signaling condition and quantum dynamics. *Physical Review Letters*, 87(17):170405, 2001. doi: 10.1103/PhysRevLett.87.170405.

[5] David E. Kaplan and Surjeet Rajendran. Causal framework for nonlinear quantum mechanics. *Physical Review D*, 105(5):055002, 2022. doi: 10.1103/PhysRevD.105.055002.

[6] William Donnelly and Laurent Freidel. Local subsystems in gauge theory and gravity. *Journal of High Energy Physics*, 2016(9):102, 2016. doi: 10.1007/JHEP09(2016)102.

[7] Laurent Freidel, Marc Geiller, and Daniele Pranzetti. Edge modes of gravity. Part I. Corner potentials and charges. *Journal of High Energy Physics*, 2020(11):026, 2020. doi: 10.1007/JHEP11(2020)026.

[8] Juan Maldacena, Douglas Stanford, and Zhenbin Yang. Conformal symmetry and its breaking in two dimensional nearly anti-de-sitter space. *Progress of Theoretical and Experimental Physics*, 2016(12):12C104, 2016. doi: 10.1093/ptep/ptw124.

[9] Douglas Stanford and Edward Witten. Fermionic localization of the Schwarzian theory. *Journal of High Energy Physics*, 2017(10):008, 2017. doi: 10.1007/JHEP10(2017)008.

[10] Phil Saad, Stephen H. Shenker, and Douglas Stanford. Jt gravity as a matrix integral. *arXiv preprint arXiv:1903.11115*, 2019.

[11] Shinsei Ryu and Tadashi Takayanagi. Holographic derivation of entanglement entropy from ads/cft. *Physical Review Letters*, 96:181602, 2006. doi: 10.1103/PhysRevLett.96.181602.

[12] Daniel L. Jafferis, Aitor Lewkowycz, Juan Maldacena, and S. Josephine Suh. Relative entropy equals bulk relative entropy. *Journal of High Energy Physics*, 2016(6):4, 2016. doi: 10.1007/JHEP06(2016)004.

[13] Nima Lashkari, Michael B. McDermott, and Mark Van Raamsdonk. Gravitational dynamics from entanglement "thermodynamics". *Journal of High Energy Physics*, 2014(4):195, 2014. doi: 10.1007/JHEP04(2014)195.

[14] Thomas Faulkner, Monica Guica, Thomas Hartman, Robert C. Myers, and Mark Van Raamsdonk. Gravitation from entanglement in holographic CFTs. *Journal of High Energy Physics*, 2014(3):51, 2014. doi: 10.1007/JHEP03(2014)051.

[15] Ahmed Almheiri, Xi Dong, and Daniel Harlow. Bulk locality and quantum error correction in ads/cft. *Journal of High Energy Physics*, 2015(4):163, 2015. doi: 10.1007/JHEP04(2015)163.

[16] Xi Dong, Daniel Harlow, and Aron C. Wall. Reconstruction of bulk operators within the entanglement wedge in gauge-gravity duality. *Physical Review Letters*, 117(2):021601, 2016. doi: 10.1103/PhysRevLett.117.021601.

[17] Daniel Harlow. The ryu-takayanagi formula from quantum error correction. *Communications in Mathematical Physics*, 354:865–912, 2017. doi: 10.1007/s00220-017-2904-z.

[18] Abhay Ashtekar, John Baez, Alejandro Corichi, and Kirill Krasnov. Quantum geometry and black hole entropy. *Physical Review Letters*, 80:904–907, 1998. doi: 10.1103/PhysRevLett.80.904.

[19] Amit Ghosh, Karim Noui, and Alejandro Perez. Statistics, holography, and black hole entropy in loop quantum gravity. *Physical Review D*, 89(8):084069, 2014. doi: 10.1103/PhysRevD.89.084069.

[20] Laurent Freidel and Simone Speziale. Twisted geometries: A geometric parametrisation of su(2) phase space. *Physical Review D*, 82:084040, 2010. doi: 10.1103/PhysRevD.82.084040.

[21] F. Peter and H. Weyl. Die Vollständigkeit der primitiven Darstellungen einer geschlossenen kontinuierlichen Gruppe. *Mathematische Annalen*, 97:737–755, 1927. doi: 10.1007/BF01447892.

[22] E. Joos and H. D. Zeh. The emergence of classical properties through interaction with the environment. *Zeitschrift für Physik B Condensed Matter*, 59(2):223–243, 1985. doi: 10.1007/BF01725541.

[23] Wojciech H. Zurek. Decoherence, einselection, and the quantum origins of the classical. *Reviews of Modern Physics*, 75(3):715–775, 2003. doi: 10.1103/RevModPhys.75.715.

[24] Erich Joos, H. Dieter Zeh, Claus Kiefer, Domenico J. W. Giulini, Joachim Kupsch, and Ion-Olimpiu Stamatescu. *Decoherence and the Appearance of a Classical World in Quantum Theory*. Springer, 2 edition, 2003. doi: 10.1007/978-3-662-05328-7.

[25] N. G. van Kampen. *Stochastic Processes in Physics and Chemistry*. North-Holland, 3 edition, 2007.

[26] Alistair Sinclair and Mark Jerrum. Approximate counting, uniform generation and rapidly mixing Markov chains. *Information and Computation*, 82(1):93–133, 1989. doi: 10.1016/0890-5401(89)90067-9.

[27] László Lovász. Random walks on graphs: A survey. In *Combinatorics, Paul Erdős is Eighty*, volume 2, pages 1–46. János Bolyai Mathematical Society, Budapest, 1993.

[28] Kenneth S. Brown. *Cohomology of Groups*, volume 87 of *Graduate Texts in Mathematics*. Springer-Verlag, 1982. doi: 10.1007/978-1-4684-9327-6.

[29] Johannes Huebschmann and Tornike Kadeishvili. Small models for chain algebras. *Mathematische Zeitschrift*, 207(1):245–280, 1991. doi: 10.1007/BF02571387.

[30] E. B. Davies. Markovian master equations. *Communications in Mathematical Physics*, 39(2):91–110, 1974. doi: 10.1007/BF01608389.

[31] Danny Birmingham, Ivo Sachs, and Sergey N. Solodukhin. Conformal field theory interpretation of black hole quasi-normal modes. *Physical Review Letters*, 88:151301, 2002. doi: 10.1103/PhysRevLett.88.151301.

[32] Subir Sachdev and Jinwu Ye. Gapless spin-fluid ground state in a random quantum Heisenberg magnet. *Physical Review Letters*, 70:3339–3342, 1993. doi: 10.1103/PhysRevLett.70.3339.

[33] Alexei Kitaev. A simple model of quantum holography. KITP Entanglement in Strongly-Correlated Quantum Matter workshop, talks on February 12 and May 7, 2015. http://online.kitp.ucsb.edu/online/entangled15/.

[34] Juan Maldacena and Douglas Stanford. Remarks on the Sachdev–Ye–Kitaev model. *Physical Review D*, 94:106002, 2016. doi: 10.1103/PhysRevD.94.106002.

[35] Jakob Yngvason. The role of type III factors in quantum field theory. *Reports on Mathematical Physics*, 55(1):135–147, 2005. doi: 10.1016/S0034-4877(05)80009-6.

[36] Venkatesa Chandrasekaran, Roberto Longo, Geoffrey Penington, and Edward Witten. An algebra of observables for de Sitter space. *Journal of High Energy Physics*, 2023(2):082, 2023. doi: 10.1007/JHEP02(2023)082.

[37] Netta Engelhardt and Aron C. Wall. Quantum extremal surfaces: holographic entanglement entropy beyond the classical regime. *Journal of High Energy Physics*, 2015(1):073, 2015. doi: 10.1007/JHEP01(2015)073.

[38] Veronika E. Hubeny, Mukund Rangamani, and Tadashi Takayanagi. A covariant holographic entanglement entropy proposal. *Journal of High Energy Physics*, 2007(7):062, 2007. doi: 10.1088/1126-6708/2007/07/062.